scientific reports

OPEN

Dynamic changes in BDNF, VEGF, and GDNF after transplanting human protein-based scaffolds with Wharton's Jelly MSCs in a rat brain injury model

Wioletta Lech[1], Marta Kot[1], Marlena Welniak-Kaminska[2], Monika Drabik[2], Leonora Buzanska[1] & Marzena Zychowicz[1]✉

Stroke poses a considerable challenge for regenerative medicine due to the complex and multidimensional specificity of the central nervous system, and cell therapy is one of the currently considered treatments. The aim of this study was to determine the pro-regenerative outcome after transplantation of preconditioned and scaffold-encapsulated mesenchymal stem/stromal cells isolated from Wharton's Jelly (WJ-MSCs) in an experimental rat model of brain injury. For this purpose, WJ-MSCs cultured at different oxygen concentrations (21% O_2 or 5% O_2) were transplanted into the injured rat brain in saline or hydrogel scaffolds derived from human platelet lysate or fibrinogen. Using magnetic resonance imaging, we observed the signal of labelled WJ-MSCs at injection site at different time-points after transplantation. By diffusion-weighted imaging we detected the signal at the lesion site only after WJ-MSCs transplantation. Furthermore, cell transplantation resulted in a significant decrease in the extent of brain damage and dynamic change in the expression of investigated rat trophic factors (BDNF, GDNF, VEGF-A) in the brain and cerebrospinal fluid. The highest increase in this expression was observed after transplantation of physioxia-preconditioned and scaffold-encapsulated cells. The results demonstrated the regenerative effect of WJ-MSCs, which was enhanced by their transplantation within human protein-based hydrogel scaffolds in the rat model of brain injury.

Stroke is a civilization disease that affects approximately 15 million people worldwide per year. It is caused by cardiac embolism, obstruction of small vessels in the brain, or atherosclerosis that affects the cerebral circulation[1] and results in transient or persistent focal cerebral ischemia. Stroke initiates a complex series of neurochemical processes, such as cell bioenergetic failure, excitotoxicity, oxidative stress, blood–brain barrier dysfunction, microcirculation damage, activation of homeostatic processes, post-ischemic inflammation, and ultimately death of neurons, glial cells, and endothelial cells[2–4]. Post-stroke inflammation causes some damage and cell death, but it simultaneously stimulates endogenous repair processes[1].

Various trophic factors, such as brain-derived neurotrophic factor (BDNF) and glial cell-derived neurotrophic factor (GDNF) are involved in the survival and differentiation of nerve cells[5] and they also play an important role in post-ischemic brain regeneration. BDNF regulates neuronal differentiation, cell survival, neurogenesis and synaptic plasticity in neurons in the peripheral and central nervous system[6,7]. Changes in BDNF expression level, both in peripheral blood and in CNS tissues, are associated with the pathogenesis of neural disorders, including ischemic stroke[7,8]. Moreover, it has been shown that BDNF is the earliest neurotrophic factor implicated in stroke in the middle cerebral artery occlusion (MCAO) ischemic model[9].

GDNF is produced by glial cells and neurons and plays an important role in neuronal differentiation during development, as well as regulating the survival, migration, and differentiation of striatal dopaminergic neurons[10]. Therefore, GDNF-dependent signalling in the striatum is essential for local dopamine release[11]. In turn, lentivirally administered GDNF was reported to induce a long-term neurological recovery in the post-acute stroke phase that was associated with brain remodelling in mice exposed to ischemia[10]. This observation is

[1]Department of Stem Cell Bioengineering, Mossakowski Medical Research Institute Polish Academy of Sciences, 5 Pawinskiego Str, 02-106 Warsaw, Poland. [2]Small Animal Magnetic Resonance Imaging Laboratory, Mossakowski Medical Research Institute Polish Academy of Sciences, 5 Pawinskiego Str, 02-106 Warsaw, Poland. ✉email: mzychowicz@imdik.pan.pl

especially important for the newborn neurons in the striatum as they were observed to die within the first weeks after ischemia[12]. In observations of damage to the central or peripheral nervous system, GDNF was also shown to promote the survival and regeneration of mature neurons, including motor and dopaminergic neurons[13].

Another trophic factor associated with stroke pathology is the vascular endothelial growth factor (VEGF). VEGF is involved in several stages of neurodevelopment, including migration, differentiation, synaptogenesis, and myelination[14,15]. In addition, VEGF stimulates vascular processes such as angiogenesis and vasculogenesis, enhancing endothelial cell proliferation and migration[16,17]. During stroke, the blood–brain barrier (BBB) is disrupted due to the loss of blood vessel-associated pericytes, thus increasing vessel permeability and causing edema. In turn, the activation of VEGF signalling during stroke was found to stimulate vascular repair mechanisms and diminish infarct size[18].

VEGF plays an important role in the regulation of the vascular endothelium by its participation in physiological and pathological neovascularization and upregulation of BBB vascular permeability to plasma proteins within minutes of exposure to ischemia[19,20]. However, the latter may cause neuroinflammation. Furthermore, it appears that the low levels of VEGF observed in a healthy adult brain are necessary for endothelial cell survival, while the higher levels observed in pathological situations are important for increased permeability and endothelial cell survival[21]. Together, these vascular processes contribute to the formation of an optimal microenvironment for neural stem cells that stimulate neuron regeneration, thereby demonstrating the important role of VEGF in the repair processes of the damaged brain[13].

Since stroke has been a major public health problem with limited treatment in recent years, the demand for novel strategies for post-stroke treatment has increased significantly[22]. Mesenchymal stem/stromal cells (MSCs) are an exceptionally promising source to be used in regenerative medicine due to their paracrine and immunomodulatory properties, as well as their specific developmental "plasticity" which enables not only mesodermal but also ectodermal differentiation in vitro[23,24]. This particularly refers to the cells isolated from postnatal tissues, including Wharton's jelly-derived MSCs (WJ-MSCs), due to their early developmental stage and the lack of expression of class II histocompatibility antigens (HLA-DR), which makes them immunologically privileged and attractive for allogeneic regenerative medicine applications[23]. MSCs can have a therapeutic effect in stroke, mainly by stimulating endogenous repair processes via the secretion of several neurotrophic factors such as BDNF, nerve growth factor (NGF), hepatocyte growth factor (HGF), VEGF, basic fibroblast growth factor (bFGF), or insulin-like growth factor 1 (IGF-1)[25,26]. The paracrine activity of MSCs has a beneficial effect on neuroregeneration, in part through interaction with neural progenitor cells (NPCs). The trophic factors secreted by MSCs stimulate astrogenesis, while oligodendrogenesis is also induced by direct contact of MSCs with NPCs[27]. Moreover, MSCs can be used as an adjuvant in combination therapies using biomaterials, drugs, and rehabilitation after stroke[22].

However, the conditions under which MSCs are prepared before transplantation and delivered to damaged tissue (called "preconditioning") can strongly influence cellular therapy outcomes. Recent studies have shown that MSCs cultures in physiological normoxia (1.5–5% O_2—physioxia), may enhance their regenerative potential by stimulating their proliferation, migration, as well as antioxidant and anti-apoptotic properties[28,29]. After transplantation, MSCs were observed to inhibit microglia activity in the brain[30]. Moreover, our previous in vitro and ex vivo experiments showed that biomimetic preconditioning of WJ-MSCs in 5% of oxygen and suspension in fibrin or platelet lysate-based hydrogels enhanced their neuroprotective properties[31]. The expression levels of all of the analysed growth factors and cytokines were up-regulated when cells were cultured in a 3D microenvironment. Moreover, the organotypic hippocampal slices after the OGD (Oxygen–Glucose Deprivation) procedure that mimics an ischemic injury co-cultured with WJ-MSCs showed a significant reduction in cell death in the CA1 region. This effect was the strongest after co-culture with cells encapsulated in hydrogels and preconditioned in physiological normoxia[31]. Therefore, the appropriate preparation of stem cells before transplantation, such as selecting the source, method of isolation, and subsequent administration to the patient, should also include preconditioning of the cells in culture conditions possibly closest to those found in vivo.

For this reason, the aim of this paper was to verify in vivo whether the regenerative potential of WJ-MSCs was enhanced by their preconditioning in physioxia (5% O_2) and by cell administration within 3D hydrogels made from human plasma-derived proteins. In the experimental rat model of ischemic stroke, we verified the parameters of the injured brain (damage area, water diffusion, signal from transplanted material), the level of rat BDNF, GDNF, and VEGF-A mRNA expression in the striatum and the protein secretion in cerebrospinal fluid (CSF) at different time points after injury and transplantation of WJ-MSCs.

Results

An overview of the experimental setup is depicted in Fig. 1a, and the timeline of the performed injury, transplantations and sample collections is shown in Fig. 1b. As a model of stroke, we used ouabain–induced rat brain injury that causes chemical blockade of the Na^+/K^+ ATP-ase pump and results in metabolic and structural changes in the brain mimicking ischemic damage. As a material for transplantation, we used human mesenchymal stem/stromal cells derived from Wharton's Jelly and cultured either in standard 2D conditions in atmospheric oxygen (21%) or preconditioned in physioxia (5% O_2)[31]. In order to deliver the cells to the animals we used either cell suspended in saline (2D) or we applied human plasma-derived proteins: fibrinogen (FB) or platelet lysate (PL) to encapsulate cells and produce scaffolds in the transplantation site. We also verified the influence of sham transplantations (saline, FB or PL alone) on tested regenerative outcomes.

Analysis of rat brain damage and WJ-MSCs distribution after transplantation

Cell labelling with iron oxide nanoparticles (SPIO) allows for their subsequent visualization and distribution analysis at different time points after transplantation. In this study, the microscopic analysis showed a high

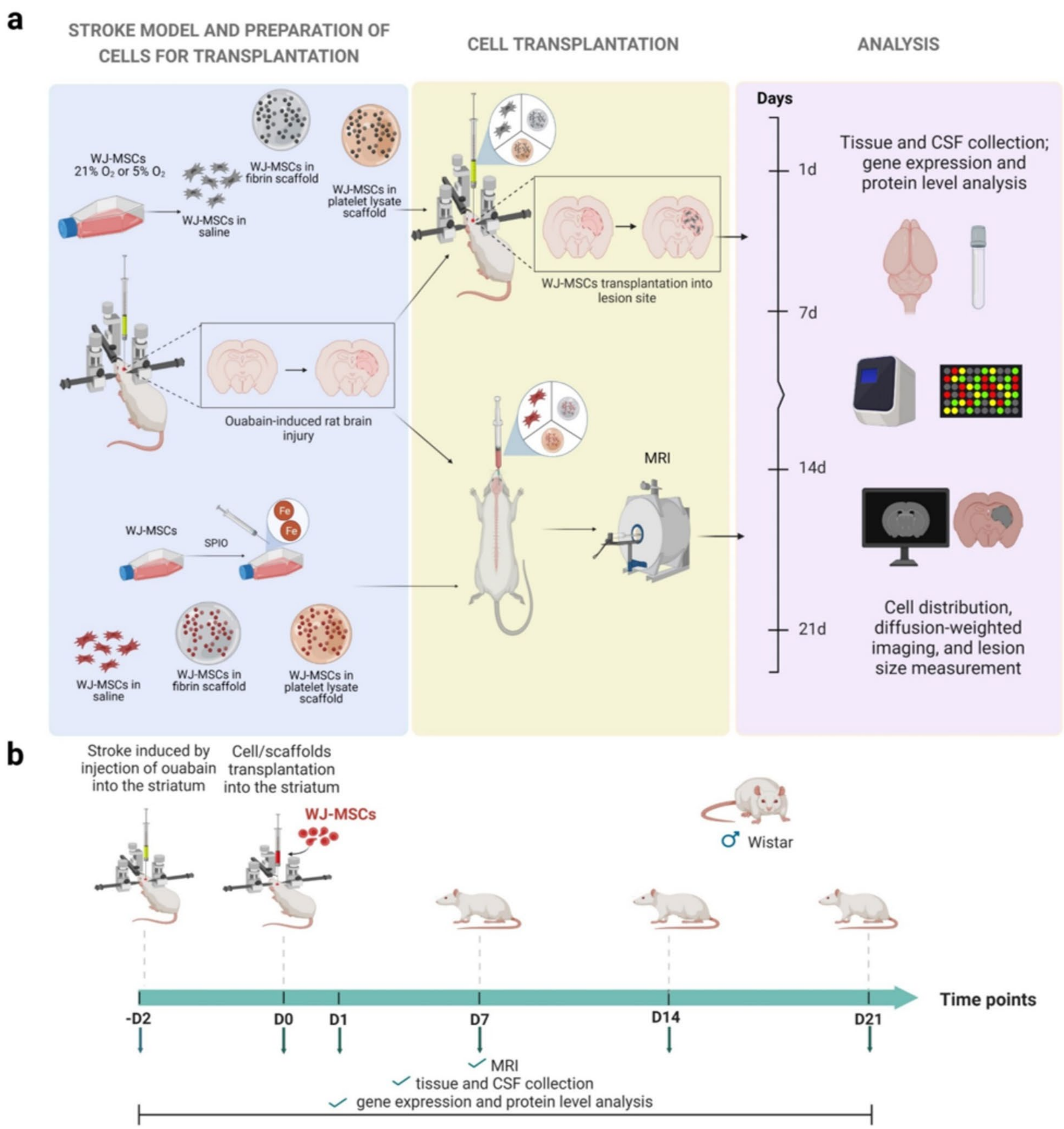

Fig. 1. The experimental setup (**a**) and timeline (**b**) of in vivo experiments. WJ-MSCs were cultured under 21% O_2 or 5% O_2 and then transplanted in saline or PL/FB scaffolds into the injured rat brain. At various time points (1, 7, 14 and 21 days), rat tissue and cerebrospinal fluid (CSF) were collected for gene expression and protein level analysis. Tissue and CSF were collected from control (non-treated) animals and after brain injury without cell transplantation, as well as after the WJ-MSCs transplantation following brain injury. For MRI analysis, WJ-MSCs cultured under 5% O_2 were labelled with SPIO and transplanted in saline (2D) or hydrogel scaffolds. At different time points (–D2, D0, D1, D7, D14, D21) after transplantation, as well as before and after brain injury without cell transplantation, animals were scanned using magnetic resonance to acquire images of the injury, cell distribution, and water diffusion. Following the scans, the areas of brain injury (lesion size) were measured. Created in BioRender. Pan, I. (2023) BioRender.com/w72h401.

efficiency of cell labelling with rhodamine B conjugated with iron oxide nanoparticles during 7-day in vitro culture under 5% O_2 in 2D as well as in PL/FB scaffolds (Fig. 2a).

Initial phantom tests were performed to determine the minimum number of cells that could be visualized and produce a sufficient signal in magnetic resonance imaging. These tests allowed us to establish the optimal number of cells for transplantation into the injured rat brain. In the MRI (T2) sequence, the brightest signal

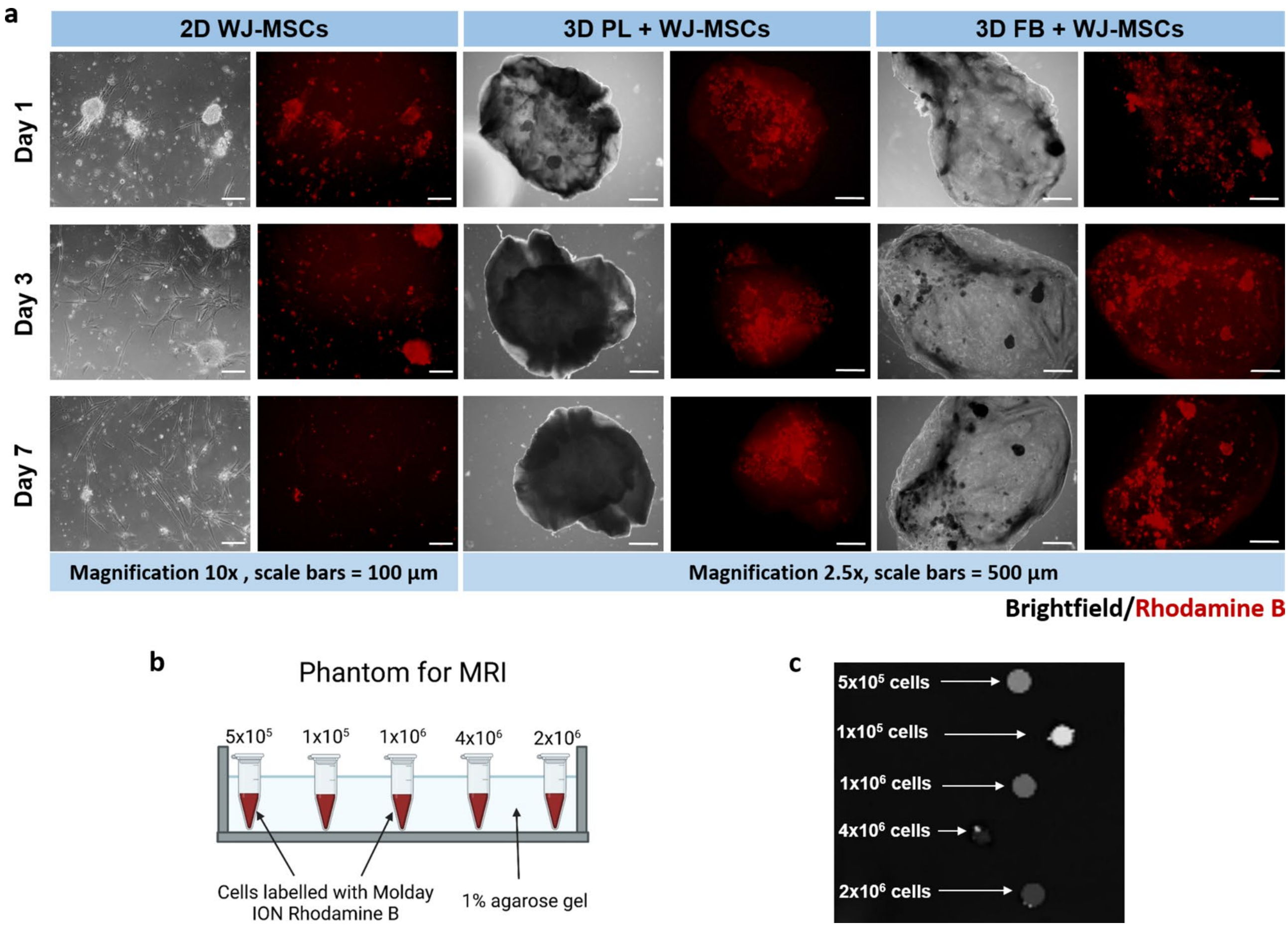

Fig. 2. In vitro analysis of WJ-MSCs in 2D or in 3D hydrogels cultured under 5% O_2. The images of cells in brightfield and labelled with superparamagnetic iron oxide nanoparticles (SPIO) conjugated with rhodamine B (red fluorescence) during a 7-day culture (**a**). Eppendorf tubes containing varying numbers of labelled cells were embedded in an agarose gel (phantom) (**b**) and visualized using MRI. The signal intensity varies based on the number of labelled cells (**c**). Scale bars = 100 and 500 µm. Created in BioRender. Pan, I. (2023) BioRender. com/w72h401 (**b**).

corresponds to the weakest signal (i.e., the lowest number of cells). As the number of cells increases, the signal becomes stronger, resulting in a darker image. Specifically, the brightest signal was observed at 1×10^5 cells (lowest number), while the darkest signal corresponded to 4×10^6 cells (highest number). Based on the phantom MRI results, the optimal number of cells for transplantation was estimated to be 5×10^5 cells (Fig. 2b,c).

After the brain injury and WJ-MSCs transplantation, as well as in the sham groups, the TurboRARE-T2 imaging and diffusion-weighted imaging were performed at different time points (24 h after transplantation, Day 7, Day 14 and Day 21) (Figs. 3, 4, 5).

After ouabain injection (OUA), brain damage in the striatum of the right hemisphere was observed (Figs. 3 and 4, red arrows). The labelled WJ-MSCs were transplanted into the lesion site (striatum) where the signal generated by the SPIO-labelled cells (black signal at the damage site) was detected 24 h later in the 2D + WJ-MSCs group, as well as in 3D PL + WJ-MSCs and 3D FB + WJ-MSCs groups (Fig. 3a, yellow arrows). The strong signal remained at a high level throughout the entire experiment (post-transplantation Day 7, Day 14 and Day 21). Interestingly, 24 h after transplantation, the labelled WJ-MSCs were only located focally in the lesion area, while on post-transplantation Day 7, 14 and 21 the signal generated by the iron oxide nanoparticles was also observed at various sites of the damaged striatum, including the site of cell administration. At this imaging resolution, no cell migration beyond the cortico-striatal lesion was observed.

The rat brain measurements performed after MRI were used to determine the extent of the striatal damage at various time points (24 h, Day 7, Day 14, and Day 21). After injection of ouabain, which mimics post-ischemic stroke changes, a loss of 32.92 ± 1.8% of the injured hemisphere (Fig. 3c) was observed and the damaged area was found to increase during ongoing experiments, at 7, 14, and 21 days time points in the OUA group (41.48 ± 2.25%, 46.95 ± 2.66% and 54.31 ± 4.03%, respectively).

A significant reduction in post-WJ-MSCs transplantation lesion size (Fig. 3c) was observed. Already 24 h after cell transplantation, a reduced damaged area in the group with cells suspended in hydrogels was observed, however, the reduction was not statistically significant (29.62 ± 0.89% for 3D PL + WJ MSCs group,

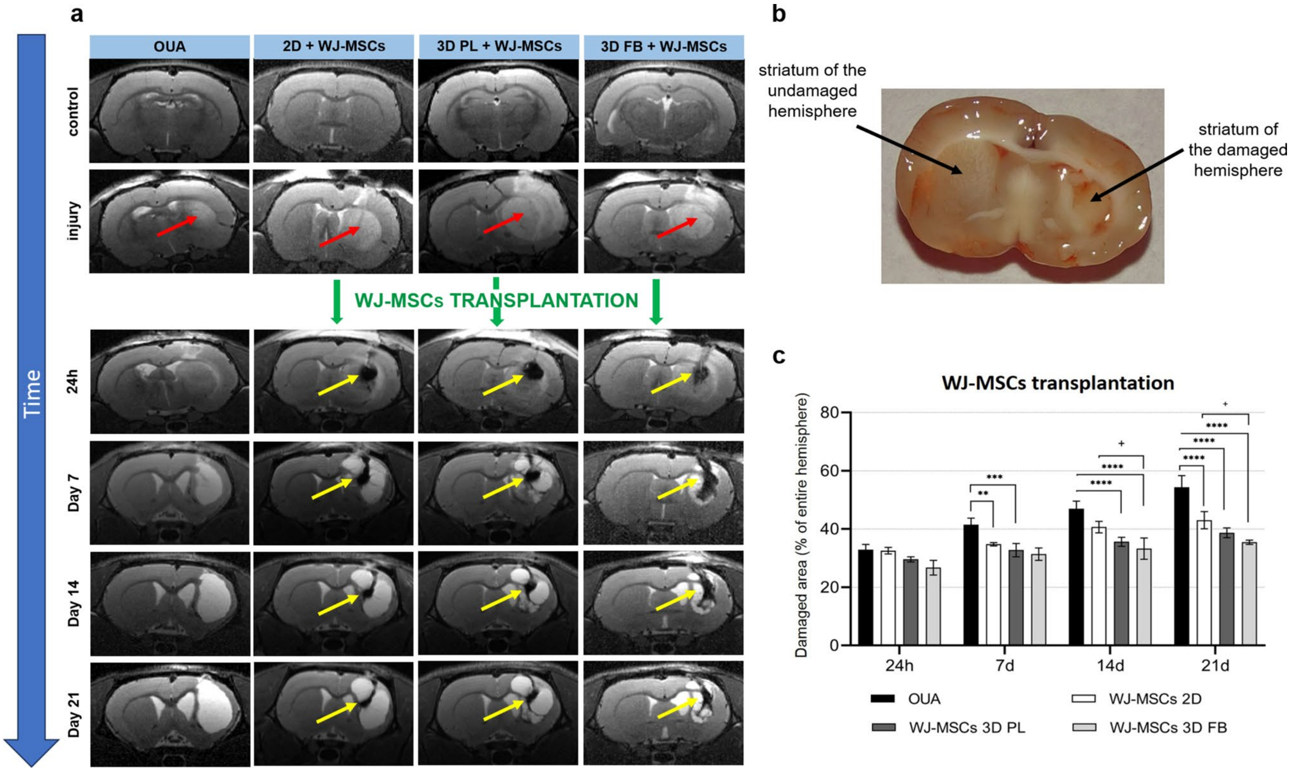

Fig. 3. MRI images of rat brains after focal injury and transplantation of WJ-MSCs cultured under 5% O_2 and suspended in saline (2D) or PL/FB scaffolds. In the striatum, damaged areas (red arrows) and transplanted WJ-MSCs labelled with iron oxide nanoparticles (yellow arrows indicating a black signal) are visible (**a**). The picture of injured hemisphere shows a decrease in volume (**b**). Volume measurements were taken at following time points: 24 h, 7, 14 and 21 days post-transplantation (**c**). Data are presented as a mean ± SD. Statistical analysis was performed using One Way ANOVA followed by Tukey's multiple comparisons test and compared to the lesion size after ouabain injection without cell/sham transplantation (n = 3, area calculated from three animals; **p < 0.01; ***p < 0.001; ****p < 0.0001; + p < 0.05), with "+" denoting statistical significance between transplantation in saline versus PL and FB scaffolds.

and 26.74 ± 2.51% for 3D FB + WJ-MSCs group) (Fig. 3c). Day 7 correlated with an increased size of the damaged area in OUA group, while the transplantation of saline-suspended cells as well as cells in PL scaffolds caused a statistically significant reduction of the damaged brain area to the values of 34.77 ± 0.59% and 32.77 ± 2.28%, respectively. The transplantation of both types of scaffolds also resulted in a statistically significant reduction in the damaged brain area measured 14 and 21 days after transplantation (35.63 ± 1.55% for 3D PL + WJ-MSCs group, and 33.26 ± 3.66% for 3D FB + WJ-MSCs group). At the last time point (Day 21) the largest post-WJ-MSCs transplantation decrease of the brain damage extent was observed in the animals that received WJ-MSCs suspended in FB scaffolds (43.04 ± 2.94% in 2D + WJ MSCs, 38.71 ± 1.66% in 3D PL + WJ MSCs, and 35.48 ± 0.73% in 3D FB + WJ MSCs group) (Fig. 3c).

In sham experiments, during the first week post-transplantation, the administration of any of the analysed vehicles (saline or PL/FB scaffolds) did not provide statistically significant protection against brain damage (Fig. 4b). However, in the following two weeks (Days 14 and 21), a reduction in lesion size was observed. Notably, a statistically significant difference was detected only in animals that received platelet lysate-based scaffolds (Fig. 4b). A comparison of the effects of cell transplantation versus sham injection on lesion size at various time points across all experimental groups revealed statistically significant differences only in animals that received cells in fibrin scaffolds (3D FB + WJ MSCs) and those that received cell-free fibrin scaffolds (FB sham). This effect was observed at all analyzed time points (24 h, Day 7, Day 14, and Day 21). Transplantation of cells encapsulated in FB scaffold led to a more pronounced reduction in lesion size compared to injection of the scaffold alone. Additionally, 21 days after WJ-MSCs transplantation or sham injection, a significant difference was observed between the 2D + WJ MSCs group and the 2D sham group, with both showing a comparable effect in reducing the injured area in the rat brain (Fig. 4c).

The diffusion-weighted imaging was also performed in the animals with transplanted cells as well as in the sham groups. As the DWI shows the directions of movement of the water molecules in the scanned tissue and the technique was used to verify the presence of water diffusion in the lesion site. After ouabain-induced brain injury (in our OUA group), a loss of diffusion was observed in the injured area (right hemisphere), while after WJ-MSCs transplantation into the striatum, a clear signal was observed in the lesion area during ongoing experiments (Fig. 5a, yellow circles). No similar results were detected at different time points after the brain

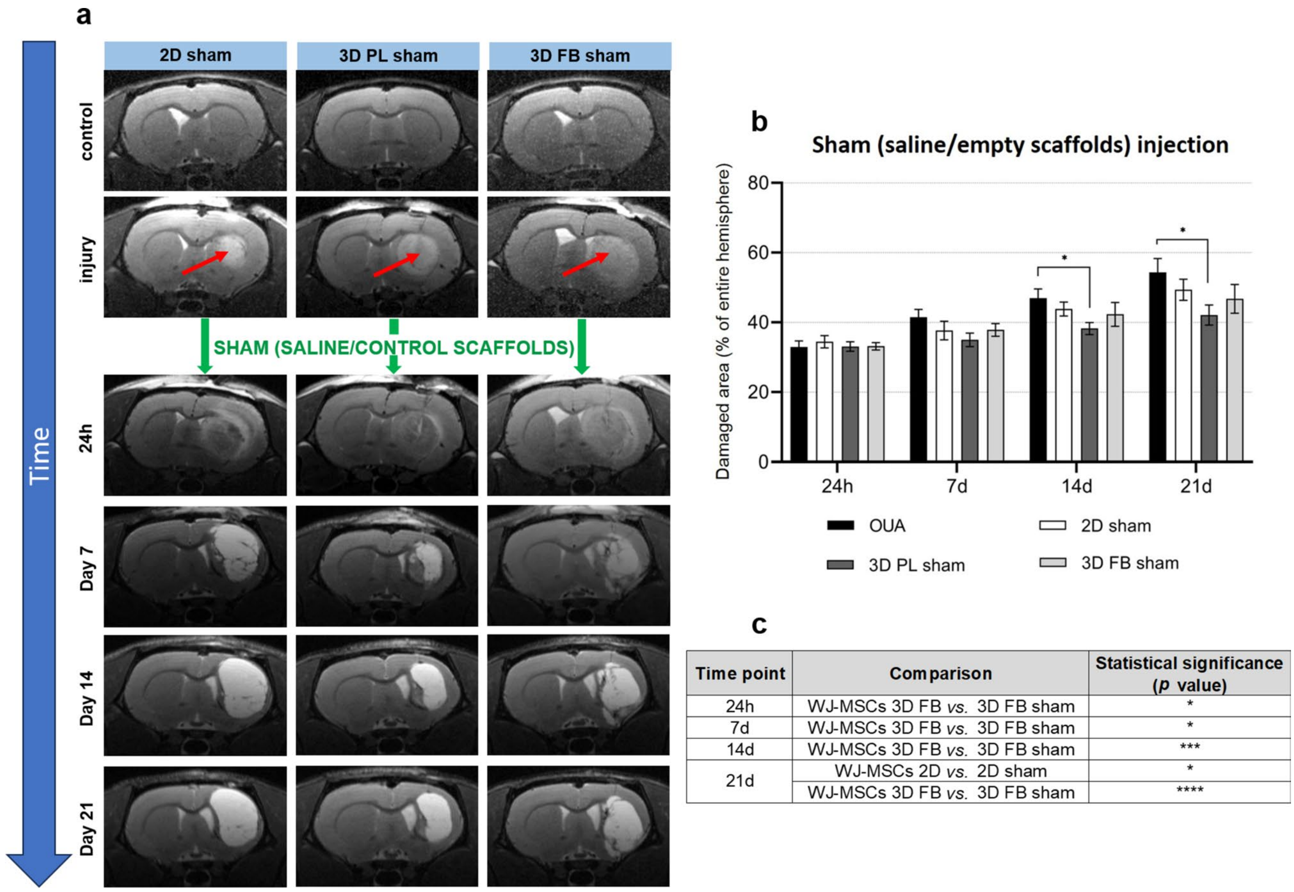

Time point	Comparison	Statistical significance (*p* value)
24h	WJ-MSCs 3D FB *vs.* 3D FB sham	*
7d	WJ-MSCs 3D FB *vs.* 3D FB sham	*
14d	WJ-MSCs 3D FB *vs.* 3D FB sham	***
21d	WJ-MSCs 2D *vs.* 2D sham	*
	WJ-MSCs 3D FB *vs.* 3D FB sham	****

Fig. 4. MRI images of rat brains following focal injury and injection of saline (2D) or PL/FB control scaffolds (sham) (**a**) and analysis of the lesion size in the sham groups (**b**). Table with statistical analysis presenting comparison of the influence of transplantation of cells encapsulated in scaffolds *versus* sham injection on the lesion size at various time points (**c**). The results are presented as a mean ± SD. Statistical analysis was performed using One Way ANOVA followed by Tukey's multiple comparisons test and compared to the lesion size after ouabain injection without cell/sham transplantation (n = 3, area calculated from three animals; *p < 0.05; ***p < 0,001; ****p < 0,0001).

injury where no WJ-MSCs were transplanted, or in 2D sham or 3D PL sham/ 3D FB sham groups (Fig. 5b), which indicates that the signal of diffusing water molecules was related to cell transplantation.

Immunohistochemical analysis of the localization iron oxide nanoparticle-labelled WJ-MSCs in the injured rat brain

The location of the WJ-MSCs transplanted in saline and platelet lysate- or fibrinogen-based scaffolds was analysed 21 days after their transplantation into the injured rat brain. The signal generated by iron oxide nanoparticles conjugated with rhodamine B was observed at the border of the cortico-striatal lesion, around the damage site in all experimental groups at Day 21 time point (Supplementary Fig. 1a–c, arrows). In the OUA group signal was not detected (Supplementary Fig. 1d). In addition, immunohistochemical analysis showed a significant loss of tissue as a result of brain damage.

Analysis of the mRNA expression of rat neurotrophic and growth factors after focal brain injury as compared to the control group

The level of mRNA expression of rat markers: BDNF, GDNF, and VEGF-A was analysed in the control group (non-treated animals) and in the study animals (after ouabain-induced injury) at 24 h, 7, 14, and 21 days' time points (Fig. 6). The evaluation of the expression level of the above markers was analysed in the striatum collected from the injured hemisphere of the study rat brains.

The most considerable increase in the expression level of all the analysed markers was detected at 24 h' time point. The elevated gene expression was sustained for BDNF for all the subsequent time points, while for GDNF and VEGF-A the increase was not statistically significant on days: 7, 14 and 21 of our analysis. At these time points a similar level of mRNA for GDNF and VEGF-A was observed, however, the level was statistically lower than at 24 h' time point (Fig. 6a–c).

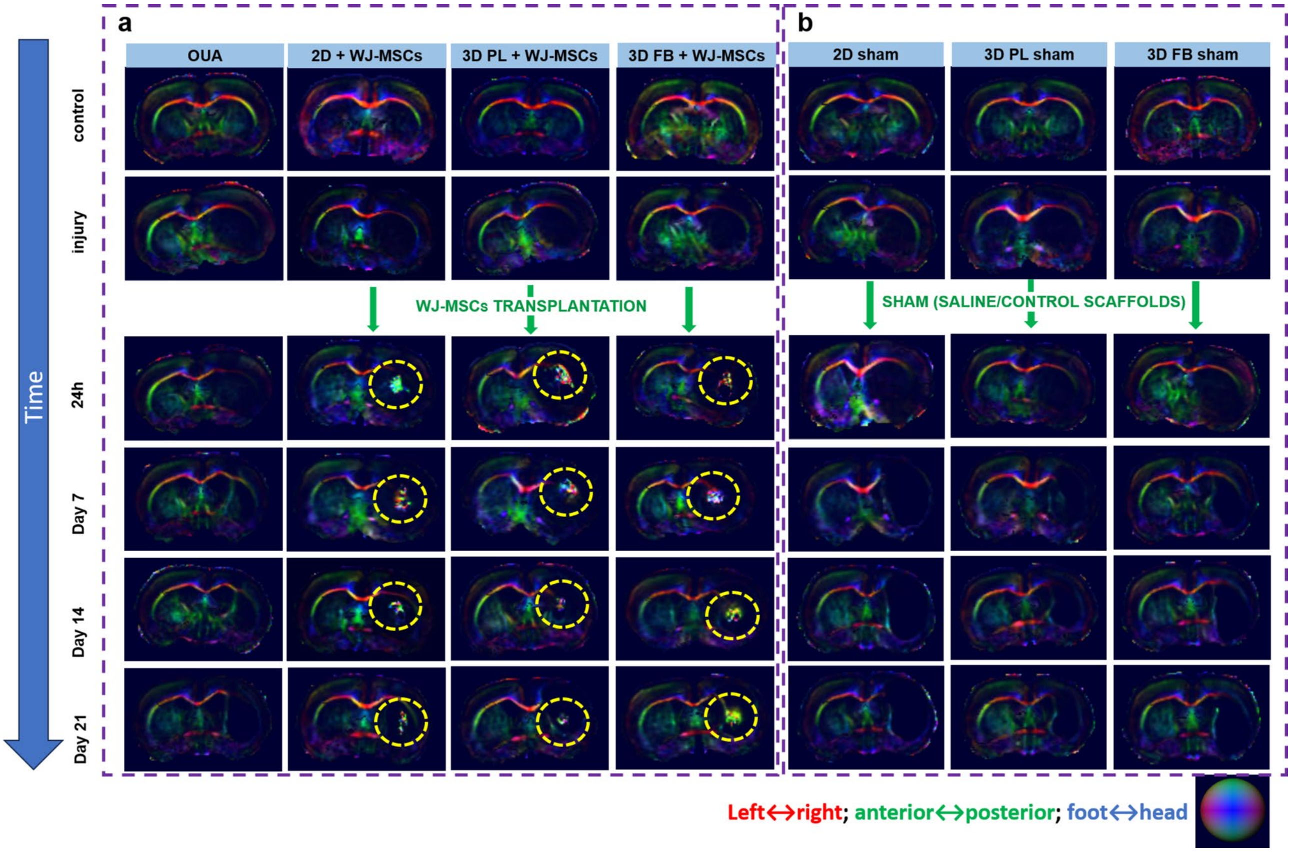

Fig. 5. MRI images of the diffusion direction of water molecules (diffusion-weighted imaging, DWI) in rat brains after transplantation into the injured animals. Rats received WJ-MSCs cultured under 5% O_2 in saline (2D) or PL/FB scaffolds (**a**) or sham injections of saline or empty PL/FB scaffolds (**b**). Diffusion directions are color-coded: red for left ↔ right, green for anterior ↔ posterior, and blue for foot ↔ head. Yellow circles highlight the signal detected during diffusion-weighted imaging at the lesion site after cell transplantation, which was absent after the injury (OUA group) (**a**), and in sham groups (**b**). Representative images were acquired from three animals per experimental group at each time point.

Analysis of the mRNA expression of rat neurotrophic and growth factors after focal brain injury and WJ-MSCs transplantation

We intended to assess whether cell preconditioning at 5% O_2 prior to transplantation and the application of hydrogel scaffolds would improve the regenerative parameters of WJ-MSCs which is the effect observed after stimulation of the mRNA expression level of host tissue-derived markers: BDNF, GDNF, and VEGF-A. These factors were analysed in the striatum collected from the injured (post-focal) hemisphere at 24 h, 7, 14, and 21 days' time points after brain damage induction and WJ-MSCs transplantation in saline (2D) or PL/FB hydrogel scaffolds, as well as in the sham groups.

Twenty-four hours after transplantation of WJ-MSCs, no increase in rat BDNF mRNA expression was observed in the injured striatum, regardless of the method of the cell administration (saline or scaffolds) and irrespective of the WJ-MSCs culture conditions before transplantation (21% O_2 vs. 5% O_2). In the following days, an increase in the level of BDNF expression was observed 7 days after cell transplantation when compared to OUA group. The same effect was observed after 14 days and was maintained on Day 21 of the observation. The WJ-MSCs administration method and in vitro culture conditions prior to transplantation did not significantly affect the expression of BDNF at 24 h and on Day 7 and Day 14. On Day 21 of our investigation the most substantial increase in mRNA expression level was observed in the animals that received PL scaffolds with WJ-MSCs previously cultured under physioxia conditions (5% O_2) (Fig. 7a).

The analysis of rat GDNF showed a tendency toward a decrease of mRNA expression level in the injured rat striatum 24 h after WJ-MSCs transplantation, regardless of the cell administration method and WJ-MSCs culture conditions before transplantation. On post cell transplantation Day 7, a change in the level of GDNF expression was observed, with statistically significant changes detected in the animals with the transplanted cells which had been preconditioned in physioxia and suspended either in saline (2D 5% O_2) or encapsulated in PL scaffolds (3D PL 5% O_2), which was not observed in OUA group. After 14 and 21 days of WJ-MSCs transplantation, a similar effect was observed: GDNF mRNA expression was maintained at a higher level than in OUA group. Furthermore, the highest levels of mRNA expression were observed in the injured rat striatum after cell transplantation in scaffolds, especially in PL-based hydrogel, as compared to saline injection. In addition, on

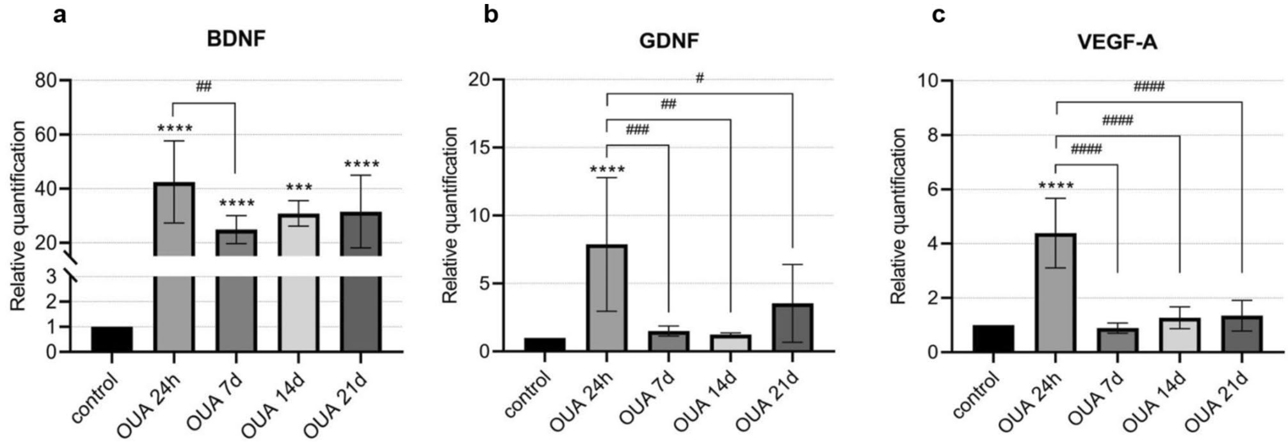

Fig. 6. Analysis of rat neurotrophic and growth factors expression at mRNA level in the injured rat brain (OUA groups) at different time points (24 h, Day 7, Day 14, and Day 21) compared to the non-treated animals (control group). The relative expression level of the analysed genes was normalized to the value of GAPDH reference gene. Results are presented as a mean ± SD, with the control group set to a value of 1. The "*" symbol indicates comparison of the statistically significant difference in expression levels in the rat brain after injury versus control. The "#" symbol indicates comparison of the expression level in the rat brain at different time points after focal injury. Statistical analysis was performed using One Way ANOVA followed by Tukey's multiple comparisons test (n = 12, samples collected from 4 animals analysed in triplicate; $^{***}p < 0.001$; $^{****}p < 0.0001$; $^{\#}p < 0.05$; $^{\#\#}p < 0.01$; $^{\#\#\#}p < 0.001$; $^{\#\#\#\#}p < 0.0001$).

the last day of the experiment, cell preconditioning under physioxia was also observed to increase the level of mRNA expression of rat GDNF in the injured striatum which was not observed in the transplanted cells grown under 21% O_2 conditions (Fig. 7b).

Twenty-four hours after WJ-MSCs transplantation, a statistically significant decrease in VEGF-A mRNA expression was observed in the injured rat striatum, regardless of the cell administration method (whether saline or hydrogel scaffolds) and WJ-MSCs culture conditions prior to transplantation (21% O_2 *vs*. 5% O_2), while from Day 7 onward, a gradual increase in VEGF-A expression levels were observed in the injured rat striatum after WJ-MSCs transplantation, which was not detected in the OUA group. Similar effects were observed 14 and 21 days after transplantation of WJ-MSCs. A statistically significant increase in VEGF-A expression was observed in all experimental groups except for the post-focal injury group and the group that received fibrinogen-based hydrogels. The in vitro WJ-MSCs culture conditions before transplantation and the method of their administration did not have a significant impact on the changes in the mRNA expression level of rat VEGF-A. A similar expression level of this growth factor was observed in all experimental groups at a later stage of stroke (Fig. 7c).

In the sham groups, no increase in the level of rat BDNF expression was observed 24 h after saline/control scaffolds injection into the injured rat brain. After 7 days, a lower level of mRNA expression was observed than after the WJ-MSCs transplantation. After 14 and 21 days, the mRNA expression level in the sham groups was comparable to the expression level observed after the WJ-MSCs transplantation (Fig. 7a).

Lower levels of mRNA expression of rat GDNF were recorded in the sham groups at 24 h, 7, 14, and 21 days after saline/control scaffolds injection than in the OUA group and the groups after saline- and hydrogel-based cell transplantation (Fig. 7b).

Twenty-four hours after saline/control scaffolds injection, a decrease in VEGF-A expression level was observed in sham groups, as opposed to OUA group. After 7, 14, and 21 days, the VEGF-A mRNA expression level in sham groups was comparable to the mRNA expression level observed after the WJ-MSCs transplantation (Fig. 7c).

Analysis of the rat neurotrophic and growth factors concentration in the cerebrospinal fluid after focal brain injury and WJ-MSCs transplantation

The concentration of rat markers: BDNF, GDNF, and VEGF-A was analysed at various time points (24 h, Day 7, Day 14, Day 21) after brain damage and WJ-MSCs transplantation. The concentration level of these proteins was analysed in the cerebrospinal fluid collected from the rat cisterna magna.

The concentration of BDNF in the rat cerebrospinal fluid after focal injury (ouabain-induced) increased significantly at each tested time point when compared to the no-injury animals (36.80 ± 10.85 pg/mL). At the 24 h, the BDNF level was recorded at 150.13 ± 92.46 pg/mL, on Day 7 at 82.80 ± 76.37 pg/mL, on Day 14 at 48.80 ± 21.17 pg/mL, and on Day 21 at 48.80 ± 22.63 pg/mL. In our sham groups an increased concentration of BDNF was observed only at 24 h' time point. After saline injection, the BDNF concentration was 106.13 ± 66.01 pg/mL, and it reached the values of 218.80 ± 121.62 pg/mL and 182.80 ± 234.76 pg/mL for PL scaffolds and FB scaffolds respectively. In the following days of analysis, the BDNF concentration observed in the animals from sham groups remained at a level similar to that observed in the controls (Fig. 8a). A significant increase in BDNF concentration was observed 24 h after WJ-MSCs transplantation, especially when cells were encapsulated and transplanted in hydrogels. At this time point the highest level of BDNF in the CSF was observed in the 3D PL 21% O_2 group (520.80 ± 246.07 pg/mL) and in the animals that received cells cultured under 5% O_2 and transplanted in FB scaffolds (455.80 ± 159.81 pg/mL). In the other experimental groups, 24 h after WJ-MSCs transplantation the concentration of BDNF amounted to: 179.47 ± 88.03 pg/mL (2D 21% O_2), 387.80 ± 159.81 pg/mL (3D FB 21% O_2), 110.81 ± 31.11 pg/mL (2D 5% O_2), and 292.80 ± 50.91 pg/mL (3D PL 5% O_2). On the next days of observation, in these experimental groups, an increase in BDNF concentration was observed as compared to the concentration in CSF after brain injury without cell transplantation. Furthermore, BDNF concentration remained at a higher level after WJ-MSCs transplantation in the scaffolds, especially in FB hydrogels, as compared to the 2D (Fig. 8a).

A decreased concentration of GDNF was recorded in post-focal injury rat CSF as compared to the level observed in the control animals (190 ± 114.90 pg/mL). At the next time points, the level of GDNF decreased, however, substantial differences within the group of animals were detected: 158.75 ± 212.13 pg/mL at 24 h, 83.75 pg/mL on Day 7, 171.25 ± 229.81 pg/mL on Day 14, and 71.25 ± 53.03 pg/mL on Day 21. The saline and control scaffolds injection resulted in an increase in GDNF concentration only 24 h after PL scaffolds transplantation (229.58 ± 191.35 pg/mL), while at subsequent time points similar or reduced GDNF concentration levels were observed in the 2D sham and 3D FB sham groups as compared to the post-focal injury groups (Fig. 8b). The transplantation of WJ-MSCs, especially in 3D, caused a significant increase of GDNF level in CSF at 24 h' time point. The highest level was observed when the cells were injected in PL scaffolds cultured in both tested oxygen conditions (546.25 ± 249.69 pg/mL for 21% O_2 and 402.50 ± 26.52 pg/mL for 5% O_2). The elevated GDNF level continued to be seen for experimental groups on the next days of observation: 7 days after WJ-MSCs transplantation, as well as 14 days after transplantation of the cells cultured under 21% O_2 conditions and then transplanted in FB scaffolds (346.25 ± 53.03 pg/mL) and WJ-MSCs cultured under 5% O_2 and transplanted in saline (308.75 ± 106.07 pg/mL). 21 days after the cell transplantation, a similar or reduced level of GDNF concentration was observed when compared to the post-focal injury groups. For some collected samples, the concentration of GDNF in the analysed CSF was below the detection level (Fig. 8b).

The VEGF-A concentration in the rat CSF after focal injury was comparable to the level observed in the control animals (78.10 ± 4.38 pg/mL). After injection of saline or control scaffolds, a lower concentration of VEGF-A was observed, particularly after 24 h. On the following days of analysis, the VEGF-A concentration detected in the animals that received saline or PL scaffolds remained at a similar level as observed in the controls (approximately 75 pg/mL). However, after injection of control FB scaffolds, the concentration of VEGF-A remained at a lower level than observed in the control group—about 65 pg/mL (Fig. 8c). The concentration of VEGF-A was recorded at a similar level (about 80 pg/mL) 24 h after WJ-MSCs transplantation in 2D and scaffolds or even lower after transplantation of the cells cultured under 21% O_2 conditions and injected in FB scaffolds (67.37 ± 3.04 pg/mL). On Day 7, the highest VEGF-A concentration was observed after transplantation of the cells cultured under 21% O_2 conditions and transplanted in saline or PL scaffolds (about 84 pg/mL), while the lowest concentration was observed after transplantation of WJ-MSCs cultured under 5% O_2 conditions and transplanted in saline or FB scaffolds (approximately 69 pg/mL). The peak of VEGF-A concentration was observed 14 days after transplantation of WJ-MSCs cultured in 21% O_2 and encapsulated in PL scaffolds (87.15 ± 9.65 pg/mL), and cells preconditioned under 5% O_2 and transplanted in FB scaffolds (87.40 ± 22.32 pg/mL). 21 days after the cell transplantation, the VEGF-A concentration remained at a similar level (about 74 pg/mL) in all experimental groups (Fig. 8c).

Discussion

The development of efficient, repeatable and safe methods of obtaining, culturing, and transplantation of stem cells increases the possibility of effective use of cell therapy in regenerative medicine. As far as cell therapy for CNS disorders is concerned, to date no reports have shown a successful regeneration of damaged tissue along with the restoration of functional nervous circuits. The positive therapeutic effect observed in clinical trials so far concerned mainly the paracrine (secretory) properties of transplanted MSCs but not their ability to differentiate and functionally integrate with damaged tissue[32]. Therefore, this study focused primarily on the potential enhancement of the pro-regenerative characteristics of MSCs. These properties can be further improved by biomimetic microenvironmental conditions, such as cell culture in 5% O_2 and a delivery to injured host tissue in the injectable biomaterial (e.g., fibrinogen or platelet lysate-derived hydrogel scaffolds). The novelty of this study lies primarily in the use of protein-based hydrogel scaffolds, which could potentially be customized for personalized therapy using patient's own plasma. Such an approach may enhance the endogenous repair mechanisms by increasing the level of regeneration-supporting growth factors. This study showed that the above-mentioned hydrogels could be injected into the injured brain in a liquid form which facilitates their adjustment and fills the lesion before cross-linking occurs. Such hydrogels can be delivered to the damaged site using minimally invasive techniques[33]. The surgical brain injury model based on ouabain injection effectively replicates key aspects of ischemic injury. Based on our findings, we demonstrated that preconditioning cells in physioxia, along with encapsulating them in hydrogel scaffolds derived from plasma proteins, positively impacts their pro-regenerative potential. No data focusing on this type of human-derived scaffolds combined with physioxia conditions are currently available. To obtain such conditions the chamber that maintains constant oxygen and CO_2 level, as well as stable temperature of 37 °C was used to prepare cells for ischemic stroke treatment. In this study, we analysed both the short-term and long-term effects of transplanted cells, not only in the injured tissue but also in the cerebrospinal fluid, to assess both local and systemic responses in the recipient tissue (Fig. 1). The MR imaging performed in all our experimental groups proved that the cells remained in the injection site, however, no WJ-MSCs migration to the other brain structures was observed (Fig. 3). This indicates that the cells remain exactly at the site of their transplantation, which produces advantageous effects

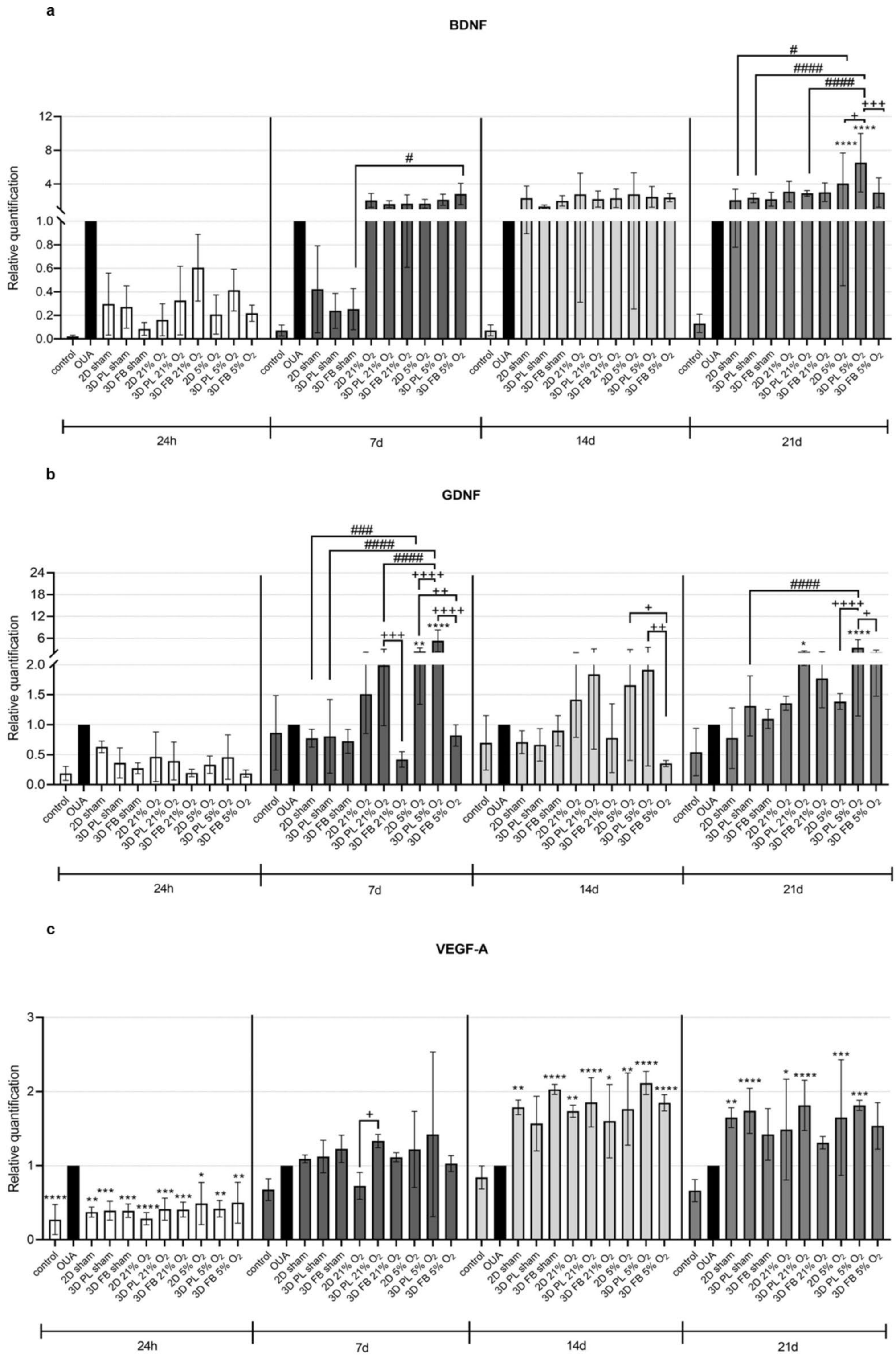

because of their paracrine neuroprotective effect. The signal generated by WJ-MSCs labelled with the iron oxide nanoparticles was detected at 1, 7, 14, and 21 days after the transplantation. Moreover, the immunohistochemical analysis confirmed localization of rhodamine B around the lesion site even on the last day of our experiment (Day 21) (Supplementary Fig. 1). Whether the signal observed in MRI came from live WJ-MSCs or from rat macrophages that phagocytosed WJ-MSCs labelled with iron nanoparticles was not the subject of this study and needs to be investigated further. However, in addition to standard MR (TurboRARE-T2 sequence) imaging we also performed diffusion-weighted imaging. This method is based on the water molecules diffusion properties in the intercellular space and allows for the stroke lesions to be detected at a very early stage[34]. Individual areas of the brain affected by ischemic changes show reduced diffusion due to changes in the permeability of cell membranes. This leads to disturbance and inhibition of Brownian motion at the stroke area and the changes can be detected in DWI[34,35]. Our DWI records revealed a loss of diffusion at the site damaged by ouabain-induced

◀**Fig. 7**. Analysis of rat neurotrophic and growth factors expression at mRNA level in injured rat brains following transplantation of WJ-MSCs cultured under 21% O_2 or 5% O_2 conditions and transplanted in saline (2D) or hydrogel scaffolds (3D PL and 3D FB), along with sham injections of saline or control scaffolds at various time points (24 h, 7, 14 and 21 days) and in the control group (non-treated animals). Relative quantification was normalized to the GAPDH reference gene. Results are presented relative to the expression level in the injured rat brain (OUA) used as a calibrator group (value = 1, statistical significance indicated by "*"). Data are shown as a mean ± SD. The "#" symbol indicates a comparison of expression levels based on the aerobic conditions under which WJ-MSCs were cultured before transplantation, while the "+"symbol indicates a comparison between different forms of WJ-MSC transplantation: either in saline or within PL/FB scaffolds. Statistical analysis was performed using One Way ANOVA followed by Tukey's multiple comparisons test (n = 12, samples collected from four animals analysed in triplicate; $^{*}p < 0.05$; $^{**}p < 0.01$; $^{***}p < 0.001$; $^{****}p < 0.0001$; $^{\#}p < 0.05$; $^{\#\#\#}p < 0.001$; $^{\#\#\#\#}p < 0.0001$; $^{+}p < 0.05$; $^{++}p < 0.01$; $^{+++}p < 0.001$; $^{++++}p < 0.0001$).

brain injury (Fig. 5). However, after WJ-MSCs transplantation in saline, PL and FB scaffolds, a clear signal was observed at the lesion site at all experimental time points and in all study groups, beside the sham groups (Fig. 5). The signal in DWI (Fig. 5, yellow circles) indicating the presence of water molecules diffusion detected in the damaged area after cell transplantation, but not in sham groups, confirms the viability of WJ-MSCs at this site in all verified experimental time points.

We also verified whether the type of transplanted material (either cells, scaffolds or biomaterial combined with WJ-MSCs) would affect the size of damaged brain area. The observed significant reduction of lesion size by transplanted WJ-MSCs (Fig. 3), especially when cells were injected in hydrogels, indicates their strong neuroprotective effect facilitating the survival of neuronal cells, particularly pronounced on day 21 of the observation (Fig. 3c). This can be explained by additional protection the transplanted cells due to their encapsulation in the scaffolds, which improved their post-transplant survival[36]. While the sham scaffold also reduced lesion size (3D PL sham vs OUA, Fig. 4a,c), incorporating WJ-MSCs into the hydrogels synergistically enhanced the positive neuroprotective effect on the penumbra area (Fig. 4c). In addition, the immunomodulatory properties of the protected WJ-MSCs can make them act effectively in the penumbra which directly surrounds the ischemic core[37]. That suggests that in that area there was no cell death which usually accompany the process of enlarging area of necrosis after the stroke. Moreover, we indicated that even control hydrogel scaffolds transplantation could have a beneficial effect on the reduction of brain damage, however, not as strong as was the case in WJ-MSCs transplantation. Similarly, the results reported by Li et al. showed that traumatic brain injury in a mice model treated with mouse BM-MSCs suspended in the injectable hydrogel scaffold, made from gelatine hydrogel cross-linked by horseradish peroxidase and choline oxidase, significantly reduced the brain damage area, alleviated neuronal inflammation and apoptosis, facilitated the survival and proliferation of endogenous nerve cells, and promoted the restoration of neurological functions[38]. The structure and composition of the scaffolds used in the sham groups differ and this can lead to varying effects on the injured brain and the tissue response. The scaffolds themselves contain a variety of components, including growth factors, cytokines, and vitamins which are absent in saline. This is clearly reflected in the differences observed in lesion size following the injection of saline versus PL/FB scaffolds. In our previous in vitro studies[31], we also observed a significant effect of the scaffolds on WJ-MSCs encapsulated inside the scaffold as well as after the indirect co-culture of cells in 2D and 3D with the organotypic hippocampal slices in the ischemic ex vivo model. In this model cells cultured in scaffolds inhibited the cell death in CA1 hippocampal region after temporary ischemic episode much more efficiently than cells cultured in 2D. This provides a strong evidence, that the scaffold could influence significantly the properties of encapsulated cells but also can affect the surrounding microenvironment. In other studies, a hydrogel consisting of sodium alginate and hyaluronic acid was used for WJ-MSCs transplantation into Sprague-Dawley rats after the traumatic brain injury. A significant restoration of the animals' motor skills was observed already 14 days after the cell transplantation. Moreover, some researchers reported their histological analysis which showed an increased presence of WJ-MSCs after their transplantation in hydrogels, which indicates that the scaffolds provided protection for transplanted cells and allowed for their migration to the lesion site[39].

After the injury, the immune, nervous and endocrine systems are mobilized, which is crucial for the proper tissue regeneration process which includes the phases of inflammation, cell proliferation and migration, tissue remodelling, and activation of e.g., macrophages and progenitor cells[40,41]. Transforming growth factor β (TGF-β), basic fibroblast growth factor (bFGF), epidermal growth factor (EGF), VEGF, IL-6, and IL-8 are some of the most important factors in this process[40,41]. The observed increase in rat BDNF, GDNF, and VEGF-A expression levels in response to the ouabain-induced injury, especially within the short timespan (24 h) (Fig. 6) indicates the initiation of an endogenous neuro- and vasculo-protective process. When comparing the expression levels of the analysed markers recorded after the cell transplantation and in the injured rat striatum where no cell therapy was applied, it can be concluded that WJ-MSCs are strongly engaged in neurorepair mechanisms directly in the injured tissue. This effect was especially marked for WJ-MSCs cultured under physioxia conditions and then transplanted in PL scaffolds, where rat BDNF and GDNF expression level increased 7 days after cell transplantation and remained at the elevated level for the next weeks of observation (post-transplantation Day 14 and Day 21) thereby suggesting a long-term activation of the endogenous repair mechanisms (Fig. 7). The elevated VEGF-A expression we observed shortly after the injury is consistent with the report by Ghori et al. (2022) (Fig. 6)[18]. Surprisingly, transplantation of WJ-MSCs lowered VEGF-A expression at 24 h time point, but then significantly increased mRNA expression for VEGF-A in the next two weeks, promoting angiogenesis and vasculogenesis (Fig. 7). Similar results were also obtained by other research groups. Torres-Espín et al.

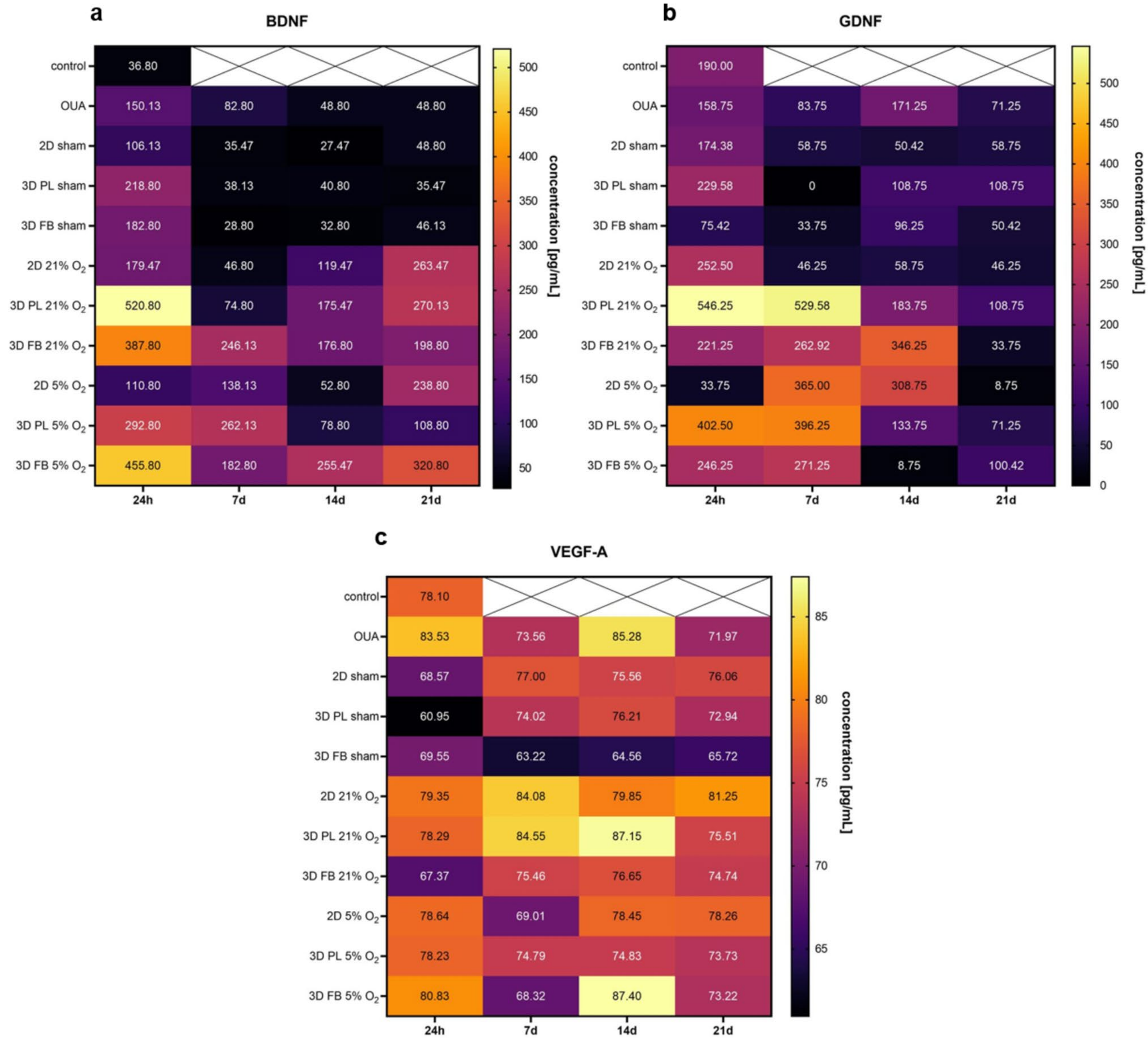

Fig. 8. A heatmap displays the concentration level of rat neurotrophic and growth factors in the cerebrospinal fluid collected at various time points (24 h, 7, 14 and 21 days) after cell transplantation. Control groups consisted of non-treated rats (control) and rats after ouabain treatment (OUA). WJ-MSCs cultured under 21% O_2 or 5% O_2 were transplanted in saline (2D) or hydrogel scaffolds (3D PL/3D FB) into the animals having ouabain-induced focal injury. The animals obtaining saline injection or cell-free scaffolds transplantation constituted the sham groups in this experiment. The results are presented as a mean ± SD. Lighter colors on the heatmaps represent higher concentrations of growth factors, while darker colors indicate lower concentrations of the analyzed markers in cerebrospinal fluid. Statistical analysis was performed using One Way ANOVA followed by Tukey's multiple comparisons test (n = 4, samples collected from four animals; *p < 0.05; **p < 0.01; ***p < 0.001). The following statistically significant differences were observed: for BDNF: control vs. 3D PL 21% O_2 24 h (***p < 0.001); control vs. 3D FB 21% O_2 24 h (*p < 0.05); control vs. 3D FB 5% O_2 24 h (**p < 0.01); OUA 24 h vs. 3D PL 21% O_2 24 h (*p < 0.05); 2D 21% O_2 24 h vs. 3D PL 21% O_2 24 h (*p < 0.05); for GDNF: 2D 21% O_2 7d vs. 3D PL 21% O_2 7d (*p < 0.05); for VEGF-A: OUA 24 h vs. 3D PL sham 24 h (*p < 0.05); OUA 14d vs. 3D FB sham 7d (**p < 0.01); 3D FB sham 14d vs. 3D FB 5% O_2 14d (*p < 0.05).

showed that BM-MSCs obtained from Sprague-Dawley rats and transplanted immediately after the spinal cord injury increased the expression of genes related to the protection and tissue regeneration. When the cells were transplanted 7 days after the injury, the decreased expression of genes related to tissue regeneration was observed. The most important change after MSCs transplantation was an increase in gene expression associated with the immune system foreign body reaction. Regarding MSCs transplantation, it was suggested that the observed therapeutic effect in spinal cord injury resulted from cells ability to secrete and/or induce the expression of protective molecules, such as BDNF and GDNF, to modulate inflammation and create a more favourable environment for axon regeneration and reconstruction of nerve tissue[42].

We have previously shown in the in vitro and ex vivo experiments that WJ-MSCs expressed certain therapeutic agents, such as growth (BDNF, GDNF, VEGF-A), and immunomodulatory (TGF-β1, IL-6, IL-1β) factors and that 5% O_2 preconditioning and mainly cell hydrogel application exerted a positive effect on the expression profile of these factors. Importantly, this profile undergoes strong changes after WJ-MSCs exposition to the injured tissue[31]. Here in our in vivo experiments, we found that cell preconditioning in physioxia can additionally alter the effect that cells in hydrogels exert on the expression of investigated trophic factors of the injured rat brain.

For further detailed verification of the recipient's response to the WJ-MSCs transplantation, the level of secreted neurotrophic and growth factors in the rat cerebrospinal fluid was assessed. Cerebrospinal fluid is involved in the physiological control of the brain and reflects the pathophysiology of various neurological disorders of the central nervous system. After the stem cell transplantation in an experimental model of stroke, quantitative analysis of the cerebrospinal fluid proteome could potentially reveal the therapeutic effect of transplanted cells on the host CNS[43]. An interesting result of the tested protein concentration in the CSF was obtained 24 h after the WJ-MSCs transplantation into the injured rat brain. The concentration of BDNF and GDNF in the CSF was observed to reach a relatively higher level than for the expression of these neurotrophins at the mRNA level in the rat striatum after treatment with WJ-MSCs (Figs. 7, 8). Several days after the stroke and WJ-MSCs transplantation, the expression of neurotrophins increases due to the activation of the regeneration process which is additionally stimulated by transplanted WJ-MSCs. The high concentration of BDNF and GDNF measured in CSF one day after cell transplantation might be the result of the body's systemic response to the local tissue damage and the induction of endogenous neurogenesis. Tan et al. showed that an increased level of BDNF in rat cerebrospinal fluid was associated with the induction of neurogenesis in the subventricular zone in response to ischemic brain injury[44]. Another group of researchers also used the same model of stroke and reported better functional regeneration and reduced rat brain damage area observed 7 and 14 days after MSCs transplantation. In post-MSCs transplantation brains a much higher expression of rat neurotrophic factors, especially VEGF 3 days after the injury, as well as EGF and bFGF 7 days after MCAO was also observed. Transplanted human MSCs induced functional improvement and neuroprotection in ischemic rats possibly by IGF-1 delivery and induction of endogenous VEGF, EGF, and bFGF in the host brain[45]. In a study by Pirzad Jahromi et al., focal brain injury was induced in rats by placing the formed clot in the central artery of the brain. Animals were injected intravenously with BM-MSCs 24 h after the stroke and sacrificed after 7 days. After BM-MSCs transplantation, the neurological result improved significantly as compared to the control group, moreover, an increase in astrocytosis, vascularization, and endogenous proliferation was observed[46]. In conclusion, the complexity of the ischemic stroke pathophysiology requires the treatment which includes a number of factors to promote tissue protection, axon repair, and functional regeneration.

In our study, the mechanism of action of the transplanted WJ-MSCs was probably based on the modulation of the host inflammatory response, and then the stimulation of endogenous cells, which ultimately resulted in accelerated process of the damaged tissue regeneration. This led to an increased expression levels of neurotrophins, such as BDNF or GDNF, and then also elevated VEGF-A expression level. The proposed mechanism is highly probable when we consider mainly the paracrine effect of the transplanted cells, rather than their differentiation and integration with the tissue. Our observations indicated that penumbra was a strategic area where the implementation of post-ischemic stroke therapy could bring the expected benefits, and the data is consistent with reports in the available literature. Nevertheless, the time span between the first symptoms and the intervention remains to be of key importance, as treatment initiation as early as possible is crucial in stroke therapy[47].

Conclusions

Development of precise in vitro culture protocols and the method for MSCs transplantation into the damaged tissue in addition to optimized selection of the MSCs source are crucial for achievement the therapeutic effect. Several factors that may increase/enhance the effectiveness of cell therapy should be considered, including cell preconditioning in appropriate spatial and oxygen conditions. The use of human protein-derived hydrogel scaffolds as carriers for stem cells are promising therapeutic approach for application in regenerative medicine. Despite the increasing application of MSCs in regenerative medicine, many mechanisms of their therapeutic action still remain unclear and require further in-depth analysis in order to make advanced therapy with stem cell-based medicinal products effective and safe for the patient.

Materials and methods

Wharton's jelly–derived mesenchymal stem cells

Human mesenchymal stem cells isolated from umbilical cord Wharton's jelly were used for the analyses of this study. The material was obtained from the Department of Obstetrics and Gynaecology of the Infant Jesus Clinical Hospital in Warsaw. Research material was collected after obtaining informed consent from mothers. The collection of the material and its use for research purposes was conducted according to the guidelines of the Declaration of Helsinki and approved by the Bioethics Committee based at the Medical University of Warsaw, 61 Zwirki i Wigury St., 02-091 Warsaw, Poland (KB/213/2016).

Experimental animals

In vivo studies were performed with the use of Wistar rats provided by the Animal Breeding House of Mossakowski Medical Research Institute. Adult males (2–3 months old, 250–280 g weight) were used for the experiments. During the experiment and between the procedures, the animals were kept in cages in the 13:11 photoperiod and had unlimited access to food and water. In the experimental cages, the following enrichment of the environment was used: additional chips of various lengths and thicknesses, nesting material in the form of cotton flakes and cocoons, pads for grinding teeth, and shelters/hiding places. Each cage contained a maximum of six rats. All procedures and studies were conformed to the rules and principles of EU directive 2010/63, reported in accordance with ARRIVE guidelines, and approved by the 1st Local Ethics Committee for Experiments on Animals based at the Faculty of Biology, University of Warsaw, 1 Miecznikowa St., 02-096 Warsaw, Poland (No. 620/2018) and the 2nd Local Ethics Committee for Experiments on Animals based at the Warsaw University of Life Sciences, 8 Ciszewskiego St., 02-786 Warsaw, Poland (No. WAW2/079/2021).

Cell isolation and culture conditions

A fragment of the umbilical cord, approximately 15–20 cm long, was collected immediately after the birth and immersed in sterile phosphate-buffered saline (PBS, Sigma-Aldrich, #D8537) with the addition of the penicillin and streptomycin solution (1%, Gibco, #15140-122). The tissues were transported to the Department of Stem Cell Bioengineering Mossakowski Medical Research Institute PAS and served as the starting material for the isolation of WJ-MSCs.

The umbilical cord was cut transversely with a scalpel into approximately 2 mm thick sections. The cylindrical tissue fragments (3 mm diameter) were excised from the Wharton's jelly area with a biopsy punch (Miltex, GmbH, #33-32-P/25) and then transferred in PBS to 6-well plates.

The fragments of the cord were cultured under standard conditions (21% O_2) or physioxia (5% O_2) in a closed system that provides constant oxygen concentration (Xvivo System, BioSpherix) in 1 mL of growth medium/well composed of: DMEM (Dulbecco Modified Eagle Medium, Macopharma, #BC0110060) supplemented with 10% human platelet lysate (Macopharma, #BC0190020), 1 mg/mL glucose (Sigma-Aldrich, #G6152), 2 U/mL heparin (Sigma-Aldrich, #H3149), and Antibiotic–Antimycotic Solution (AAS, 1%, Gibco, #15240062).

When the WJ-MSCs migrated from the explant and reached 70% confluence, the cultures were passaged using an accutase solution (Accutase Cell Detachment Solution, Becton Dickinson, #561527). The cells were centrifuged for 3 min at 1000 rpm, and then the cultures were established by seeding cells in successive passages at a density of 2×10^3 cells/cm^2. The growth medium was changed every 2 days, culture conditions were maintained at 21% O_2 and 5% O_2, as described before.

The experimental model of cytotoxic brain injury

Focal rat brain injury was performed using microinjection of 5 nmol ouabain octahydrate solution (Sigma-Aldrich, #O3125) in sterile saline following the protocol described previously by the researchers from MMRI PAS[48–50]. After general anaesthesia by intraperitoneal injection of a mixture of ketamine (80 mg/kg, Bioketan, Vetoquinol Biowet Poland) and xylazine (8 mg/kg, Xylapan, Vetoquinol Biowet Poland) the rats were placed in the stereotaxic apparatus (Stoelting) and further operations were performed using the OPMI Pico (Zeiss) operating microscope. The scalp and soft tissues were cut from the eye line to the *lambda* point, then the *bregma* point was marked and a 0.5 cm diameter trepanation hole was drilled above the right hemisphere of the brain following the coordinates [X (0.5); Y (3.8); Z (4,7)] to the *bregma* point and based on the stereotaxic atlas. A Hamilton needle coupled with a precision syringe was inserted into the rat brain, and then microinjection of 1 µL of 5 nmol ouabain solution was performed using an infusion pump (Stoelting). The substance was injected at a rate of 1 µL/min to the striatum of the right hemisphere of the rat brain according to the coordinates [X (0.5); Y (3.8); Z (4.7)]. The needle was left in the brain for 2 min to prevent fluid backflow and then carefully withdrawn from the brain and the edges of the wound on the skin were sealed with a surgical suture (Dafilon, 5/0, DS16, Braun, #C0932124). After the procedure, an antibiotic—enrofloxacin (5 mg/kg, Baytril, Bayer Veterinary, Poland) and an analgesic—meloxicam (5 mg/kg, Metacam, Boehringer Ingelheim, Vetmedica GMBH) were injected subcutaneously.

Preparation of WJ-MSCs and their transplantation into the injured rat brain

WJ-MSCs at 3rd–5th passage cultured under 21% O_2 or 5% O_2 conditions were detached with accutase, washed twice with PBS, centrifuged (1000 rpm, 3 min.), and then 5×10^5 cells were prepared for transplantation to the injured rat brain. Forty-eight hours after the ouabain-induced brain damage, the animals were anesthetized by intraperitoneal administration of a mixture of ketamine (80 mg/kg), and xylazine (8 mg/kg) and then placed in a stereotaxic apparatus (Stoelting). After skin disinfection and removal of stitches placed after the brain injury performed previously, the microinjection of mesenchymal stem cells was performed into the striatum of the right hemisphere of the rat brain. WJ-MSCs were transplanted either as encapsulated in hydrogel scaffolds (3D) or suspended in saline (2D). The scaffolds were made from thrombin cross-linked human platelet lysate (PL) (Macopharma), or human plasma fibrinogen (FB) (5 mg/mL, Sigma-Aldrich, #F3879). Thrombin (Sigma-Aldrich, #T6884) was diluted in Tris-buffered saline (TBS, Sigma-Aldrich, #T5030) with the addition of $CaCl_2$ (ThermoFisher Scientific, #L13191) to a final concentration of 2 U/mL thrombin and 250 µM $CaCl_2$. The scaffolds were prepared immediately prior to cell transplantation into the rat brain. For this purpose, 30 µL of thrombin solution was dropped into a Petri dish and mixed with 30 µL of WJ-MSCs suspended in platelet lysate or fibrinogen with the addition of aprotinin (10 µg/mL, Sigma-Aldrich, #A1153). 60 µL of WJ-MSCs in a hydrogel mixture or saline suspension were immediately withdrawn by syringe inserted into the rat brain and half the volume injected to prevent air from entering. The cells were transplanted according to the stereotaxic coordinates [X (0.5); Y (3.8); Z (4.7)] in the injured area of the brain. For sham groups, only saline or cell-free scaffolds were transplanted. After transplantation, the edges of the wound were joined with a surgical thread. Animals were injected subcutaneously with antibiotic—enrofloxacin 5 mg/kg and analgesic—meloxicam 5 mg/kg.

Estimation of cell number for magnetic resonance imaging

To visualize transplanted cells using magnetic resonance imaging (MRI), WJ-MSCs cultured under 5% O_2 were labelled with rhodamine-conjugated iron oxide nanoparticles – Molday ION Rhodamine B (Biopal, #CL-50Q02-6A-50) at a concentration of 20 µg/mL added to the medium for 24 h before cell transplantation. In the first step, the labelling efficiency was assessed in vitro. The cells were seeded in 6-well plates, labelled with Molday ION Rhodamine B for 24 h, fixed with 4% paraformaldehyde (PFA, Sigma-Aldrich, #158127) for 15 min, washed three times with PBS, and then visualized using an Axio Vert.A1 (Zeiss) fluorescence microscope. Then, to establish the optimal number of cells visible in MRI after transplantation to animals, a preliminary examination was performed using a phantom to determine the number of cells that generated the signal. 1×10^5, 5×10^5, 1×10^6, 2×10^6, and 4×10^6 cells labelled for 24 h were used to measure the signal. A phantom (a container filled with 1% agarose gel) was used to stabilize the tubes and prevent air artefacts. Tubes with a different number of cells were subjected to magnetic resonance imaging (Biospec 70/30 USR 7 T, Bruker).

Magnetic resonance imaging

Magnetic resonance imaging was performed using a Bruker BioSpec 70/30 Avance III 7 T system. Radiofrequency (RF) excitation was performed using a cylindrical, quadrature RF coil (8.6 cm internal diameter). A separate receive-only coil was used for data acquisition—a phased array coil (2 × 2 elements) dedicated to rat brain imaging placed directly over the animal's head. Rats after brain injury and WJ-MSCs cultured under 5% O_2 transplantation in saline (2D) or hydrogels (PL/FB scaffolds) were scanned at different time points: 24 h, 7, 14, and 21 days after transplantation. The animals were anesthetized with isoflurane (4% for induction, 1.5–2% in oxygen for maintenance provided through a mask) and placed on a scanning bed in a prone position with the head attached to a stereotaxic apparatus (Bruker). The respiratory rate and body temperature were monitored throughout the experiment using a small animal monitoring system (SA Instruments). Positioning scans were performed, followed by a high-resolution TurboRARE T2-weighted scan with the following parameters: repetition time (TR) = 5000 ms (ms), echo time (TE) = 15 ms, effective echo time (TEeff) = 30 ms, RARE factor = 4, number of averages = 3, spatial resolution = 0.125 × 0.125 mm, slice thickness = 0.5 mm, interslice distance = 0.5 mm, the number of slices = 54, acquisition matrix = 256 × 256, flip angle (FA) = 180, acquisition time (TA) = 12 min 15 s. Diffusion-weighted imaging was performed using echo-planar imaging diffusion tensor imaging (EPI-DTI) sequence with parameters: TR = 3750 ms, TE = 33 ms, number of averages = 1, spatial resolution = 0.156 × 0.172 mm, slice thickness = 1.0 mm, interslice distance = 1.5 mm, the number of slices = 5, acquisition matrix = 192 × 128, TA = 8 min 45 s, number of B0 images = 5, diffusion directions = 30, number of segments = 4, diffusion gradient duration = 7.5 ms, diffusion gradient separation = 12 ms, bvalue = 670 s/mm^2. Imaging was performed in Small Animal Magnetic Resonance Imaging Laboratory, Mossakowski Medical Research Institute, Polish Academy of Sciences.

Rat brain damage analysis

Brain measurements were performed using 3D Slicer software v. 4.11.20210226 (https://www.slicer.org/). Measurements of the area of the entire damaged hemisphere and the size of the ouabain-induced brain injury expressed in mm^3 were made, and then the percentage of the area of the hemisphere that underwent cytotoxic damage over the entire hemisphere was determined. Brains after focal injury (ouabain-induced) and WJ-MSCs transplantation in 2D and scaffolds, as well as after injection of saline or sham scaffolds were analysed at subsequent time points (24 h, 7-, 14- and 21-days post-transplantation). Additionally, the DTI data was reconstructed and visualized using Paravision 5.1 software (Bruker), resulting in diffusion direction maps.

Cerebrospinal fluid collection

Cerebrospinal fluid was collected from anaesthetized rats after injury (before stem cell transplantation) and then 1, 7, 14, and 21 days after transplantation. Samples collected from rats without brain injury were served as a control group. The animals were anaesthetized by intraperitoneal administration of a mixture of ketamine (80 mg/kg), and xylazine (8 mg/kg) according to their body weight. After anaesthesia, the rats were placed in a stereotaxic apparatus (Stoelting) with the head positioned at a 45° angle. The skin was disinfected, and the needle was inserted into the anterior occipital membrane between the basal part of the occipital bone and the anterior arch of the apical vertebrae. Cerebrospinal fluid (approximately 100–150 µL) was withdrawn by syringe straight from the cisterna magna through a needle to a sterile 200 µL Eppendorf tubes and stored at -80 °C until analysis. Only the samples that were not contaminated with blood were analysed.

Tissue collection

The animals were sacrificed by decapitation and then the brains were isolated. The rat brains were cut with a scalpel in the transverse plane in 1/3 of their length, and the striatum from the damaged hemisphere of the brain was collected for further analysis. The tissues were frozen on dry ice and then stored at -80 °C until gene expression level analysis. The whole brains of animals were placed in 50 mL falcon tubes filled with 4% PFA and left for 24 h at 4 °C. The next day, the brains were placed in a 30% sucrose solution (Sigma-Aldrich, #S9378) containing 0.1% sodium azide (Sigma-Aldrich, #S2002). After 24 h, the brains were frozen on dry ice and stored at -80 °C for subsequent immunohistochemical analysis.

Immunohistochemical analysis of the lesion site

The WJ-MSCs were labelled with iron oxide nanoparticles—Molday ION Rhodamine B (20 µg/mL) before transplantation into the striatum of the rat brain. After performing MR imaging, the animals were decapitated and the whole brains were collected. The material was obtained from rats 21 days after the ouabain-induced injury (OUA group) and after the stem cells in saline or PL/FB scaffolds were transplanted into the injured striatum. 24 h before the brain slicing procedure, the tissue was transferred to − 20 °C environment. The frozen brains were cut into 20-µm sections with a cryostat and mounted on silane-coated slides. The slides were stored for further analysis at − 80 °C.

The tissue slices were fixed with 4% PFA for 20 min at room temperature for immunohistochemical analysis. After washing with PBS (Gibco, #18912-014), the cell nuclei were stained with 5 µM Hoechst 33258 (Sigma-Aldrich, #94403) for 20 min at room temperature. After rinsing with PBS, Fluorescent Mounting Medium (Dako, #S302380-2) was added to the slides and then covered with glass coverslips. For image acquisition, the preparations were analysed using a LSM 780 confocal system (Zeiss), Cell Observer SD system (Zeiss) equipped with the Axio Observer Z.1 microscope, and Zen 2012 software (Zeiss). Visualizations were performed in Laboratory of Advanced Microscopy Techniques, Mossakowski Medical Research Institute, Polish Academy of Sciences.

Quantitative reverse transcription polymerase chain reaction (RT-PCR) analysis

The striatum samples collected from the animals were kept on dry ice. mRNA was isolated using Fenozol Reagent (Total RNA Mini Plus, A&A Biotechnology, #036-100) after tissue homogenization with a manual homogenizer. The obtained samples were treated with 1 U/mL DNase (Clean-Up RNA Concentration, A&A Biotechnology, #039-100C), and the mRNA purity was evaluated using a NanoDrop One Microvolume UV–Vis spectrophotometer (ThermoFisher Scientific). The High-Capacity RNA-to-cDNA Kit (Applied Biosystems, #4387406) was used for the preparation of cDNA, according to the manufacturer's protocol. Quantitative RT-PCR (qRT-PCR) was performed with the cDNA samples using the 7500 Real-Time PCR System (Applied Biosystems), SYBR Green PCR Master Mix (Life Technologies, #4364344), and gene-specific primers (Supplementary Table 1) with the following program: one step at 50 °C for 2 min, polymerase activation at 95 °C for 10 min, 40 cycles of denaturation at 95 °C for 15 s and 40 cycles of annealing, extension, and read fluorescence at 60 °C for 1 min, cooling at 4 °C at the end of reaction. mRNA expression levels were calculated using the $2^{-\Delta\Delta Ct}$ method. The GAPDH expression level was used as an internal control to calculate the expression level of the analysed rat genes. qRT-PCR was performed on the samples prepared from 4 animals in three replicates.

Immunoenzymatic analysis

The analysis was carried out in the cerebrospinal fluid collected from control animals, from the rats after focal injury (OUA group), the rats after transplantation of WJ-MSCs suspended in saline (2D + WJ-MSCs) or encapsulated in 3D PL (3D PL + WJ-MSCs) /3D FB (3D FB + WJ-MSCs) scaffolds, and the animals with injected saline (2D sham)/control scaffolds (3D PL sham and 3D FB sham) at 24 h, 7, 14, and 21 days' time points. Two-fold diluted cerebrospinal fluid was used for the analysis. Rat BDNF ELISA Kit (Sigma-Aldrich, #RAB1138-1KT), and Rat GDNF ELISA Kit (Sigma-Aldrich, #RAB1144-1KT) were used to analyse the concentration of neurotrophins (BDNF and GDNF) in the rat cerebrospinal fluid. A Rat Premixed Multi-Analyte Kit (R&D Systems, #LXSARM-03) was used to analyse the VEGF-A concentration. The absorbance was measured at 450 nm with a FLUOstar Omega plate reader (BMG LABTECH) (for BDNF and GDNF), and the VEGF-A concentration was measured using a Bio-Plex 200 system (Bio-Rad).

Statistics

Statistical evaluation was based on a minimum of 3–6 independent experiments. Statistical analysis was performed using the GraphPad Prism 9 software. Mean ± standard deviation (SD) was calculated for all samples and we applied the Shapiro–Wilk normality test prior to performing analysis of variance (ANOVA). The statistical significance was determined using ANOVA followed by Tukey's multiple comparisons test. A value of $p < 0.05$ was considered significant.

Data availability

All data are available upon request (wlech@imdik.pan.pl).

Received: 17 July 2023; Accepted: 23 May 2025
Published online: 02 July 2025

References

1. Maida, C. D., Norrito, R. L., Daidone, M., Tuttolomondo, A. & Pinto, A. Neuroinflammatory mechanisms in ischemic stroke: Focus on cardioembolic stroke, background, and therapeutic approaches. *Int. J. Mol. Sci.* **21**(18), 6454. https://doi.org/10.3390/ijms21186454 (2020).
2. Brouns, R. & De Deyn, P. P. The complexity of neurobiological processes in acute ischemic stroke. *Clin. Neurol. Neurosurg.* **111**(6), 483–495. https://doi.org/10.1016/j.clineuro.2009.04.001 (2009).
3. Zong, P., Lin, Q., Feng, J. & Yue, L. A systemic review of the integral role of TRPM2 in ischemic stroke: From upstream risk factors to ultimate neuronal death. *Cells* **11**(3), 491. https://doi.org/10.3390/cells11030491 (2022).
4. Hu, X. et al. Role of glial cell-derived oxidative stress in blood-brain barrier damage after acute ischemic stroke. *Oxid. Med. Cell. Longev.* **2022**, 7762078. https://doi.org/10.1155/2022/7762078 (2022).
5. Kurtzeborn, K., Cebrian, C. & Kuure, S. Regulation of renal differentiation by trophic factors. *Front. Physiol.* **9**, 1588. https://doi.org/10.3389/fphys.2018.01588 (2018).
6. Bathina, S. & Das, U. N. Brain-derived neurotrophic factor and its clinical implications. *Arch Med Sci.* **11**(6), 1164–1178. https://doi.org/10.5114/aoms.2015.56342 (2015).
7. Eyileten, C. et al. The relation of the brain-derived neurotrophic factor with MicroRNAs in neurodegenerative diseases and ischemic stroke. *Mol. Neurobiol.* **58**(1), 329–347. https://doi.org/10.1007/s12035-020-02101-2 (2021).
8. Dou, S. H., Cui, Y., Huang, S. M. & Zhang, B. The role of brain-derived neurotrophic factor signaling in central nervous system disease pathogenesis. *Front. Hum. Neurosci.* **16**, 924155. https://doi.org/10.3389/fnhum.2022.924155 (2022).

9. Kokaia, Z. et al. Regulation of brain-derived neurotrophic factor gene expression after transient middle cerebral artery occlusion with and without brain damage. *Exp. Neurol.* **136**(1), 73–88. https://doi.org/10.1006/exnr.1995.1085 (1995).
10. Beker, M. et al. Lentivirally administered glial cell line-derived neurotrophic factor promotes post-ischemic neurological recovery, brain remodeling and contralesional pyramidal tract plasticity by regulating axonal growth inhibitors and guidance proteins. *Exp. Neurol.* **331**, 113364. https://doi.org/10.1016/j.expneurol.2020.113364 (2020).
11. Chermenina, M. et al. GDNF is important for striatal organization and maintenance of dopamine neurons grown in the presence of the striatum. *Neuroscience* **270**, 1–11. https://doi.org/10.1016/j.neuroscience.2014.04.008 (2014).
12. Arvidsson, A., Collin, T., Kirik, D., Kokaia, Z. & Lindvall, O. Neuronal replacement from endogenous precursors in the adult brain after stroke. *Nat. Med.* **8**(9), 963–970. https://doi.org/10.1038/nm747 (2002).
13. Wagenaar, N. et al. Promoting neuroregeneration after perinatal arterial ischemic stroke: Neurotrophic factors and mesenchymal stem cells. *Pediatr. Res.* **83**(1–2), 372–384. https://doi.org/10.1038/pr.2017.243 (2018).
14. Rosenstein, J. M., Krum, J. M. & Ruhrberg, C. VEGF in the nervous system. *Organogenesis* **6**(2), 107–114. https://doi.org/10.4161/org.6.2.11687 (2010).
15. Carmeliet, P. & Ruiz de Almodovar, C. VEGF ligands and receptors: implications in neurodevelopment and neurodegeneration. *Cell Mol. Life Sci.* **70**(10), 1763–1778. https://doi.org/10.1007/s00018-013-1283-7 (2013).
16. Schlieve, C. R. et al. Vascular endothelial growth factor (VEGF) bioavailability regulates angiogenesis and intestinal stem and progenitor cell proliferation during postnatal small intestinal development. *PLoS ONE* **11**(3), e0151396. https://doi.org/10.1371/journal.pone.0151396 (2016).
17. Muratori, L. et al. Evaluation of Vascular Endothelial Growth Factor (VEGF) and its family member expression after peripheral nerve regeneration and denervation. *Anat. Rec. (Hoboken).* **301**(10), 1646–1656. https://doi.org/10.1002/ar.23842 (2018).
18. Ghori, A. et al. Vascular endothelial growth factor augments the tolerance towards cerebral stroke by enhancing neurovascular repair mechanism. *Transl. Stroke Res.* **13**(5), 774–791. https://doi.org/10.1007/s12975-022-00991-z (2022).
19. Zhang, Z. G. et al. VEGF enhances angiogenesis and promotes blood–brain barrier leakage in the ischemic brain. *J. Clin. Invest.* **106**(7), 829–838. https://doi.org/10.1172/JCI9369 (2000).
20. Weis, S. M. & Cheresh, D. A. Pathophysiological consequences of VEGF-induced vascular permeability. *Nature* **437**(7058), 497–504. https://doi.org/10.1038/nature03987 (2005).
21. Maharaj, A. S., Saint-Geniez, M., Maldonado, A. E. & D'Amore, P. A. Vascular endothelial growth factor localization in the adult. *Am. J. Pathol.* **168**(2), 639–648. https://doi.org/10.2353/ajpath.2006.050834 (2006).
22. Incontri Abraham, D., Gonzales, M., Ibarra, A. & Borlongan, C. V. Stand alone or join forces? Stem cell therapy for stroke. *Expert Opin. Biol. Ther.* **19**(1), 25–33. https://doi.org/10.1080/14712598.2019.1551872 (2019).
23. Kaundal, U., Bagai, U. & Rakha, A. Immunomodulatory plasticity of mesenchymal stem cells: A potential key to successful solid organ transplantation. *J. Transl. Med.* **16**, 31. https://doi.org/10.1186/s12967-018-1403-0 (2018).
24. Kulus, M. et al. Mesenchymal stem/stromal cells derived from human and animal perinatal tissues-origins, characteristics, signaling pathways, and clinical trials. *Cells* **10**(12), 3278. https://doi.org/10.3390/cells10123278 (2021).
25. Cunningham, C. J., Redondo-Castro, E. & Allan, S. M. The therapeutic potential of the mesenchymal stem cell secretome in ischaemic stroke. *J. Cereb. Blood Flow Metab.* **38**(8), 1276–1292. https://doi.org/10.1177/0271678X18776802 (2018).
26. Guo, Y., Peng, Y., Zeng, H. & Chen, G. Progress in mesenchymal stem cell therapy for ischemic stroke. *Stem Cells Int.* **2021**, 9923566. https://doi.org/10.1155/2021/9923566 (2021).
27. Oppliger, B. et al. Mesenchymal stromal cells from umbilical cord Wharton's jelly trigger oligodendroglial differentiation in neural progenitor cells through cell-to-cell contact. *Cytotherapy* **19**(7), 829–838. https://doi.org/10.1016/j.jcyt.2017.03.075 (2017).
28. Lan, Y. W. et al. Hypoxia-preconditioned mesenchymal stem cells attenuate bleomycin-induced pulmonary fibrosis. *Stem Cell Res. Ther.* **6**(1), 97. https://doi.org/10.1186/s13287-015-0081-6 (2015).
29. Cruz, F. F. & Rocco, P. R. M. Hypoxic preconditioning enhances mesenchymal stromal cell lung repair capacity. *Stem Cell Res. Ther.* **6**, 130. https://doi.org/10.1186/s13287-015-0120-3 (2015).
30. Hu, C. & Li, L. Preconditioning influences mesenchymal stem cell properties in vitro and in vivo. *J. Cell Mol. Med.* **22**(3), 1428–1442. https://doi.org/10.1111/jcmm.13492 (2018).
31. Lech, W. et al. Biomimetic microenvironmental preconditioning enhance neuroprotective properties of human mesenchymal stem cells derived from Wharton's Jelly (WJ-MSCs). *Sci. Rep.* **10**, 16946. https://doi.org/10.1038/s41598-020-74066-0 (2020).
32. Foo, J. B. et al. Comparing the therapeutic potential of stem cells and their secretory products in regenerative medicine. *Stem Cells Int.* **2021**, 2616807. https://doi.org/10.1155/2021/2616807 (2021).
33. Lynch, C. R., Kondiah, P. P. D. & Choonara, Y. E. Advanced strategies for tissue engineering in regenerative medicine: A biofabrication and biopolymer perspective. *Molecules* **26**(9), 2518. https://doi.org/10.3390/molecules26092518 (2021).
34. Bammer, R. Basic principles of diffusion-weighted imaging. *Eur. J. Radiol.* **45**(3), 169–184. https://doi.org/10.1016/s0720-048x(02)00303-0 (2003).
35. Baliyan, V., Das, C. J., Sharma, R. & Gupta, A. K. Diffusion weighted imaging: Technique and applications. *World J. Radiol.* **8**(9), 785–798. https://doi.org/10.4329/wjr.v8.i9.785 (2016).
36. Collins, M. N. et al. Emerging scaffold- and cellular-based strategies for brain tissue regeneration and imaging. *In Vitro Models.* **1**, 129–150. https://doi.org/10.1007/s44164-022-00013-0 (2022).
37. Li, H. et al. Immunomodulatory functions of mesenchymal stem cells in tissue engineering. *Stem Cells Int.* **2019**, 9671206. https://doi.org/10.1155/2019/9671206 (2019).
38. Li, J. et al. Dual-enzymatically cross-linked gelatin hydrogel promotes neural differentiation and neurotrophin secretion of bone marrow-derived mesenchymal stem cells for treatment of moderate traumatic brain injury. *Int. J. Biol. Macromol.* **187**, 200–213. https://doi.org/10.1016/j.ijbiomac.2021.07.111 (2021).
39. Zhang, K. et al. Potential application of an injectable hydrogel scaffold loaded with mesenchymal stem cells for treating traumatic brain injury. *J. Mater. Chem. B.* **6**(19), 2982–2992. https://doi.org/10.1039/C7TB03213G (2018).
40. Sharma, P., Kumar, A., Dey, A. D., Behl, T. & Chadha, S. Stem cells and growth factors-based delivery approaches for chronic wound repair and regeneration: A promise to heal from within. *Life Sci.* **268**, 118932. https://doi.org/10.1016/j.lfs.2020.118932 (2021).
41. Dolati, S. et al. Prospects for the application of growth factors in wound healing. *Growth Factors* **38**(1), 25–34. https://doi.org/10.1080/08977194.2020.1820499 (2020).
42. Torres-Espín, A., Hernández, J. & Navarro, X. Gene expression changes in the injured spinal cord following transplantation of mesenchymal stem cells or olfactory ensheathing cells. *PLoS ONE* **8**(10), e76141. https://doi.org/10.1371/journal.pone.0076141 (2013).
43. Hur, J. W. et al. Label-free quantitative proteome profiling of cerebrospinal fluid from a rat stroke model with stem cell therapy. *Cell Transpl.* **30**, 9636897211023474. https://doi.org/10.1177/09636897211023474 (2021).
44. Tan, X. D., Liu, B., Jiang, Y., Yu, H. J. & Li, C. Q. Gadd45b mediates environmental enrichment-induced neurogenesis in the SVZ of rats following ischemia stroke via BDNF. *Neurosci. Lett.* **745**, 135616. https://doi.org/10.1016/j.neulet.2020.135616 (2021).
45. Wakabayashi, K. et al. Transplantation of human mesenchymal stem cells promotes functional improvement and increased expression of neurotrophic factors in a rat focal cerebral ischemia model. *J. Neurosci. Res.* **88**(5), 1017–1025. https://doi.org/10.1002/jnr.22279 (2010).
46. Pirzad Jahromi, G. et al. Multipotent bone marrow stromal cell therapy promotes endogenous cell proliferation following ischemic stroke. *Clin. Exp. Pharmacol. Physiol.* **42**(11), 1158–1167. https://doi.org/10.1111/1440-1681.12466 (2015).

47. Sodaei, F. & Shahmaei, V. Identification of penumbra in acute ischemic stroke using multimodal MR imaging analysis: A case report study. *Radiol. Case Rep.* **15**(10), 2041–2046. https://doi.org/10.1016/j.radcr.2020.07.066 (2020).
48. Dabrowska, S. et al. Human bone marrow mesenchymal stem cell-derived extracellular vesicles attenuate neuroinflammation evoked by focal brain injury in rats. *J. Neuroinflam.* **16**(1), 216. https://doi.org/10.1186/s12974-019-1602-5 (2019).
49. Jablonska, A. et al. Short-lived human umbilical cord-blood-derived neural stem cells influence the endogenous secretome and increase the number of endogenous neural progenitors in a rat model of lacunar stroke. *Mol. Neurobiol.* **53**(9), 6413–6425. https://doi.org/10.1007/s12035-015-9530-6 (2016).
50. Gornicka-Pawlak, E. B. et al. Systemic treatment of focal brain injury in the rat by human umbilical cord blood cells being at different level of neural commitment. *Acta Neurobiol. Exp. Wars.* **71**(1), 46–64. https://doi.org/10.55782/ane-2011-1822 (2011).

Acknowledgements
We are very thankful to prof. Dorota Sulejczak from Department of Experimental Pharmacology MMRI PAS for analysis of protein levels in rat CSF and to Laboratory of Advanced Microscopy Techniques MMRI PAS for assistance with Confocal Microscopy Imaging.

Author contributions
W.L.: conceptualisation, methodology, investigation, data acquisition and analysis, writing-original draft; M.K.: analysis, investigation, writing-original draft; M.W-K.: resources, investigation; M.D.: resources, investigation; L.B.: writing-review, editing, supervision; M.Z.: conceptualization, analysis, writing-original draft, editing.

Funding
The work was supported by National Science Centre Grant No. 2019/35/N/NZ5/03723 and Statutory Funds to MMRI PAS.

Declarations

Competing interests
The authors declare no competing interests.

Additional information
Supplementary Information The online version contains supplementary material available at https://doi.org/10.1038/s41598-025-04269-w.

Correspondence and requests for materials should be addressed to M.Z.

Reprints and permissions information is available at www.nature.com/reprints.

Publisher's note Springer Nature remains neutral with regard to jurisdictional claims in published maps and institutional affiliations.